Limnol. Oceanogr., 59(3), 2014, 769–787

doi:10.4319/lo.2014.59.3.0769

Distinct pools of dissolved iron-binding ligands in the surface and benthic boundary layer of the California Current

Randelle M. Bundy,[1,*] Dondra V. Biller,[2] Kristen N. Buck,[3] Kenneth W. Bruland,[2] and Katherine A. Barbeau [1]

[1] Scripps Institution of Oceanography, University of California San Diego, La Jolla, California
[2] University of California, Santa Cruz, Ocean Sciences Department, Santa Cruz, California
[3] Bermuda Institute of Ocean Sciences, Ferry Reach, St. George's, Bermuda

Abstract

Organic dissolved iron (dFe)–binding ligands were measured by competitive ligand exchange–adsorptive cathodic stripping voltammetry (CLE-ACSV) at multiple analytical windows (side reaction coefficient of salicylaldoxime, $\alpha_{Fe(SA)_2} = 30, 60$, and 100) in surface and benthic boundary layer (BBL) samples along the central California coast during spring and summer. The weakest ligands were detected in the BBL at the lowest analytical window with average log $K^{cond}_{FeL,Fe'} = 10.2 \pm 0.4$ in the summer and 10.8 ± 0.2 in the spring. Between 3% and 18% of the dFe complexation in the BBL was accounted for by HS, which were measured separately in samples by ACSV and may indicate a source of dFe-binding ligands from San Francisco Bay. The strongest ligands were found in nearshore spring surface waters at the highest analytical window with average log $K^{cond}_{FeL,Fe'} = 11.9 \pm 0.3$, and the concentrations of these ligands declined rapidly offshore. The ligand pools in the surface and BBL waters were distinct from each other based on principal components analysis, with variances in the BBL ligand pool explained by sample location, and variance in surface waters explained by water mass. The use of multiple analytical window analysis elucidated several distinct iron-binding ligand pools, each with unique distributions in the central California Current system.

Dissolved iron (dFe) concentrations in coastal oceanic surface waters are relatively low (generally < 0.5 nmol L^{-1}; Johnson et al. 1997; Biller et al. 2013). This is due to biological uptake (Johnson et al. 2007) and the low solubility of dFe in seawater (Hudson et al. 1992). The presence of organic dFe-binding ligands has been shown to increase the solubility of dFe in seawater (Rue and Bruland 1995; Wu and Luther 1995), but their sources and sinks are still not well known (*see* reviews by Hunter and Boyd 2007; Gledhill and Buck 2012). In general, strong dFe-binding ligands (L_1, log $K^{cond}_{FeL,Fe'} \geq 12.0$) measured in the surface ocean are thought to be biologically produced (Hunter and Boyd 2007; Gledhill and Buck 2012) and may play an important role in the biologically labile pool of dFe, although weaker dFe–ligand complexes (L_2, log $K^{cond}_{FeL,Fe'} < 12.0$) may be more bioavailable (Hutchins and Bruland 1994; Poorvin et al. 2011).

Weak ligand sources may include photochemical degradation of strong ligands in the surface ocean (Barbeau 2006), biological products (Hutchins and Bruland 1994; Boyd et al. 2010; Hassler et al. 2011), humic-like substances (HS; Laglera and van den Berg 2009), and diffusive fluxes from sediment pore waters and resuspended sediment material (Skrabal et al. 1997; Jones et al. 2011). However, dFe complexation is thought to be governed by stronger ligands in surface waters (Rue and Bruland 1995; *see* review by Hunter and Boyd 2007), whereas weaker complexes dominate the deep ocean "ligand soup" (Hunter and Boyd 2007).

The central and northern California Current (CC) has been well studied with respect to seasonal dFe dynamics (Johnson et al. 1999; Elrod et al. 2004; Biller et al. 2013). The CC is an eastern boundary upwelling system, with high primary productivity along the coast generally coinciding with seasonal upwelling events (Bruland et al. 2001). These periodic upwelling events may bring elevated concentrations of macronutrients (nitrate, phosphate, silicate) without a corresponding adequate increase in dFe (Bruland et al. 2001; Johnson et al. 2001; Biller et al. 2013), leading to varying degrees of iron stress in the phytoplankton community (Hutchins et al. 1998; King and Barbeau 2012).

In previous studies, the highest dFe and dissolvable Fe (weak acid labile) were found just after the onset of upwelling (Elrod et al. 2004; Chase et al. 2005; Biller et al. 2013), with fine-grained sediments deposited from rivers during winter storms as a significant source of the dissolved and particulate Fe (Elrod et al. 2008). These mud belt shelf sediments are rich in organic carbon and Fe (Homoky et al. 2012), and data from flux chambers (Berelson et al. 2003; Elrod et al. 2004) show a correlation between dFe fluxes and organic matter degradation, suggesting the Fe-rich deposits underlying the benthic boundary layer (BBL; Johnson et al. 1999) are organic in nature. Buck et al. (2007) found high concentrations of dFe-binding ligands in one BBL sample near San Francisco Bay, and it has subsequently been shown in a study of the Satilla River Estuary in the southeastern United States that sediment pore waters can be a source of dFe and ligands to the water column (Jones et al. 2011). Organic ligands may, thus, play a significant role in remobilizing upwelled dFe-rich BBL

* Corresponding author: rmbundy@ucsd.edu

Table 1. Classes of ligands used in this study where the stronger ligand classes are represented by L_1 and L_2, and the weaker ligands are represented by L_3 and L_4. Literature range represents the range of conditional stability constants reported for that ligand class in the literature, as reported by Gledhill and Buck (2012).

Ligand category	L_i	Log K	Literature range
Strong	L_1	≥12.0	9.6–13.90
	L_2	11.0–11.9	9.6–11.95
Weak	L_3	10.0–10.9	—
	L_4	≤10.0	—

material in the CC region and in determining its availability to phytoplankton in the surface ocean. Several studies have also characterized the distribution and in situ dynamics of dFe-binding organic ligands in the surface waters of the CC (Macrellis et al. 2001; Buck et al. 2007; King et al. 2012).

The purpose of this study was to investigate seasonal characteristics of both stronger and weaker dFe-binding ligands in the northern and central CC, with emphasis on surface waters compared with the BBL over the midshelf mud belts (50–90 m deep). dFe-binding ligands were measured by competitive ligand exchange–adsorptive cathodic stripping voltammetry (CLE-ACSV) using multiple concentrations of the added ligand salicylaldoxime (SA) to create a range of competition strengths of the added ligand, defined as multiple analytical windows (MAWs). This methodology allows the detection of a wider range of dFe-binding ligand classes than is determined in a single window. This MAW CLE-ACSV approach has been employed for copper (Cu) speciation studies (Bruland et al. 2000) in estuarine (Moffett et al. 1997; Buck and Bruland 2005; Ndung'u 2012) and coastal environments (van den Berg et al. 1990; van den Berg and Donat 1992; Bundy et al. 2013), although it has not yet been applied to Fe speciation studies. Recently, "reverse" titrations have been employed in one study to assess tightly bound dFe fractions not typically exchangeable with SA (Hawkes et al. 2013).

Previous studies report an overlapping range of conditional stability constants (log $K^{\mathrm{cond}}_{\mathrm{FeL,Fe'}}$) of dFe-binding ligands detected by CLE-ACSV in the marine environment (9.6–13.9; *see* table 1 in review by Gledhill and Buck 2012), confounding the distinction between the stronger "L_1" and weaker "L_2" ligand classes. This makes the interpretation of the sources and sinks of dFe-binding organic ligands in the environment difficult. The overlapping range also suggests that there may be additional ligand classes present in seawater. This study aimed to detect a wider range of dFe-binding ligand classes in surface and BBL waters using MAW analyses in the spring and summer off northern and central California. Surface waters, hypothesized to contain the strongest dFe-binding ligands, and BBL waters suspected to contain organic degradation products, terrestrial HS, or both were intended to represent two end members in ligand composition for which to verify MAW analyses for dFe-binding ligands.

Methods

Sampling—Surface and BBL samples for this study were collected on the R/V *Point Sur* in May 2010 (spring) and August and September 2011 (summer) off the coast of northern and central California (Fig. 1). All BBL stations during the August and September 2011 cruise were also sampled in the surface, whereas only a subset of BBL stations were sampled in surface waters during the May 2010 cruise (Fig. 1). Trace metal clean samples from the BBL in May 2010 and August 2011 were collected using Teflon-coated 8 liter GO-Flo bottles (General Oceanics) suspended on a Kevlar line and triggered with Teflon messengers. Hydrographic data was collected using the ship's rosette system, which contained a conductivity, temperature, and depth (CTD) sensor as well as a fluorometer, dissolved oxygen sensor, and transmissometer. The BBL sampling locations were determined based on the local maximum in-beam attenuation within 10 m of the ocean bottom, along with a higher salinity and lower temperature feature obtained from a CTD cast immediately preceding the GO-Flo cast. An attempt was made to obtain the GO-Flo sample approximately 5 m off the bottom within the BBL. Nitrate and silicic acid data for the GO-Flo sample was also used for comparison with the preceding CTD cast to ensure the sample was within the BBL. For additional details on hydrographic and trace metal sampling, *see* Biller et al. (2013). Surface samples on both cruises were obtained from a trace metal clean towed "fish" (Bruland et al. 2005) plumbed through clean Teflon tubing into a clean van for sample collection. All dissolved samples were filtered through Acropak 200 capsule filters (0.2 μm, VWR International) into bottles that had been cleaned by both nitric acid (HNO_3^-; trace metal grade, Fisher Scientific) and hydrochloric acid (HCl; trace metal grade, Fisher Scientific). Samples for total dFe were filtered into 125 mL low-density polyethylene bottles (Nalgene) and subsequently acidified to pH 2 (Lohan et al. 2006; Johnson et al. 2007). Samples collected for dFe speciation were filtered into 500 mL fluorinated polyethylene bottles (Nalgene) and either kept at 4°C for "fresh" analysis shipboard (within 1–3 d) or frozen at −20°C for later analysis (1–2 months) in the lab.

Chlorophyll a *and nutrient analyses*—Nutrients were analyzed shipboard using a Lachat QuickChem 800 Flow Injection Analysis System following standard colorimetric methods (Biller et al. 2013). Samples were analyzed for nitrate + nitrite (herein referred to as nitrate, NO_3^-), phosphate (PO_4^{3-}), and silicic acid ($Si(OH)_4$) on surface transects, as well as from GO-Flo bottles (Biller et al. 2013). Chlorophyll *a* (Chl *a*) was calculated from in situ fluorescence based on a calibrated underway data acquisition (UDAS) fluorometer (SeaBird Electronics).

dFe totals—dFe totals were determined shipboard using flow injection analysis (FIA) as described previously by Lohan et al. (2006) and in detail for this study by Biller et al. (2013). Samples were acidified to pH 2 immediately

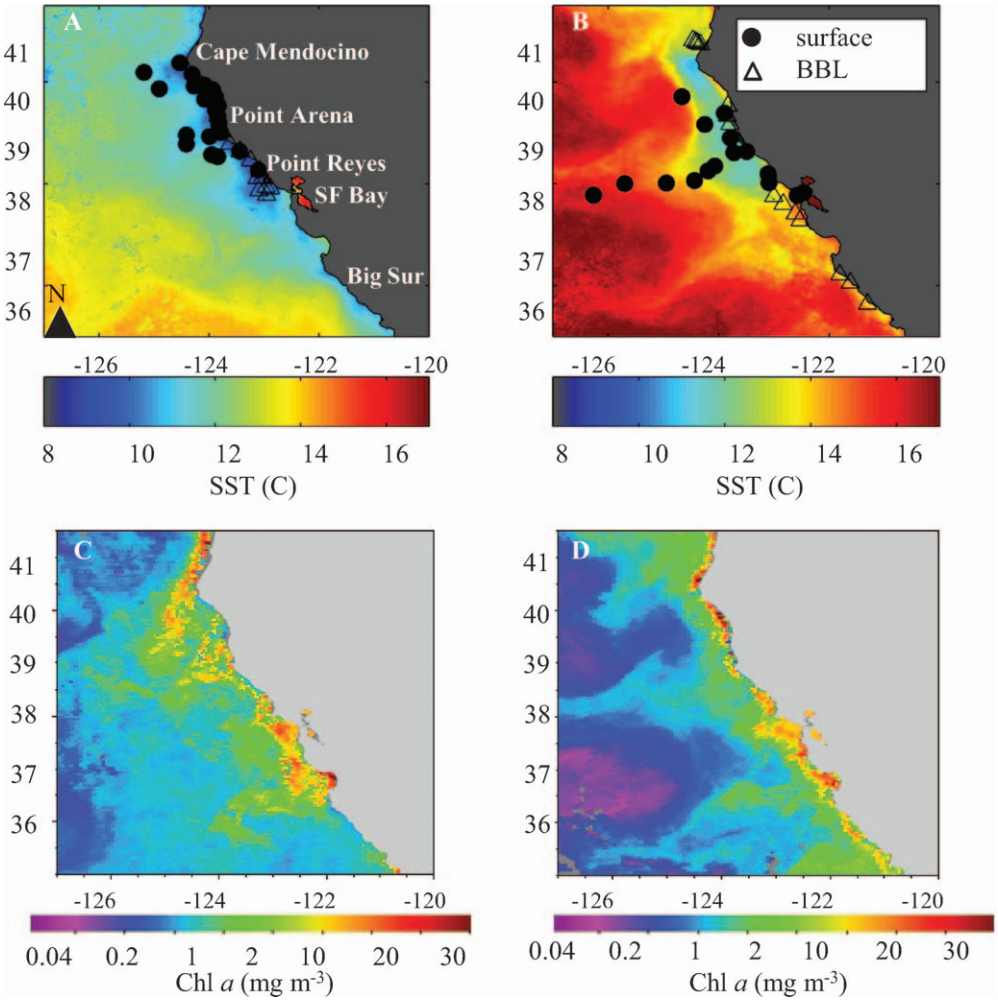

Fig. 1. Sampling stations in the surface and benthic boundary layer (BBL) during the (A) spring and (B) summer. (B) BBL stations in the summer were also sampled in the surface waters. Stations are overlaid on a one-month average (A, B), sea surface temperature (NOAA Coast Watch, °C), and (C, D) Chl *a* (NOAA Coast Watch, mg L^{-1}) for (A, C) spring and (B, D) summer cruises (May and August for spring and summer, respectively).

after collection using quartz-distilled HCl (Optima, Fisher Scientific) and were allowed to sit for 2 h before analysis. Blank measurements using this method were 0.048 ± 0.009 nmol kg^{-1} (n = 18), and the detection limit (three times the standard deviation of the blank) was 0.026 nmol kg^{-1}. As quality control, the analysis of Sampling and Analysis of Fe standards (SAFe, Johnson et al. 2007) were completed during the cruise. The results for dFe during the May 2010 cruise were surface (S1): 0.095 ± 0.006, deep (D2): 0.93 ± 0.07 (n = 11) and for the August 2011 cruise were S1: 0.094 ± 0.008 nmol kg^{-1}, D2: 0.94 ± 0.06 nmol kg^{-1} (n = 18; Biller et al. 2013). These values are in the range of the current consensus values as of May 2013 of S1: 0.093 ± 0.008 nmol kg^{-1} and D2: 0.93 ± 0.02 nmol kg^{-1} (http://www.geotraces.org/science/intercalibration/322-standards-and-reference-materials). A subset of samples were also analyzed using a new multi-element method developed by Biller and Bruland (2012) to compare with FIA results, and good agreement was seen between methods (Biller et al. 2013).

dFe speciation—dFe organic speciation was measured using CLE-ACSV with SA as the competing ligand (Rue and Bruland 1995; Buck et al. 2007), using MAWs (*see* description below). All summer samples and a subset of spring samples were analyzed with MAWs ($\alpha_{Fe(SA)_2}$ = 30, 60, 100) with a single titration at each window; remaining spring samples were analyzed in triplicate at $\alpha_{Fe(SA)_2}$ = 60 only. For the titrations, 10 mL aliquots of each dFe speciation sample were pipetted into 10 separate Teflon vials that had been preconditioned with the added dFe concentrations used in this study. A 1.5 mol L^{-1} boric acid (> 99.99%, Alfa Aeasar) buffer was prepared in 0.4 mol L^{-1} NH_4OH (Optima, Fisher Scientific), and 50 μL was added to each vial (7.5 mmol L^{-1} final concentration, pH 8.2). Eight of the 10 aliquots were then spiked with Fe from a 100 nmol L^{-1}, 200 nmol L^{-1}, 1 μmol L^{-1}, 2 μmol L^{-1}, or 10 μmol L^{-1} secondary standard that had been diluted from an AA standard (CertiPrep) into pH 1.8 ultraclean water (Milli-Q water, > 18 meg Ω cm) to obtain a final concentration ranging from 0.25 to 100 nmol L^{-1}. The

added Fe was then left to equilibrate with the natural ligands for at least 2 h, and up to 8 h. The appropriate concentration of the competing ligand was added ($\alpha_{Fe(SA)_2}$ of 30, 60, or 100) after the 2 h equilibration period with the added Fe and left to equilibrate an additional 15 min for the highest analytical window ($\alpha_{Fe(SA)_2} = 100$), and 30 min for the lower analytical windows ($\alpha_{Fe(SA)_2} = 30, 60$). Each Teflon cup was then run separately using a controlled growth mercury electrode (BAS*i*) interfaced with an analyzer (E2, Epsilon) and a laptop computer using ACSV as described in detail elsewhere (Rue and Bruland 1995; Buck et al. 2007, 2010). The calibration of the side reaction coefficient ($\alpha_{Fe(SA)_2}$) for SA has been completed previously according to Rue and Bruland (1995) with corrections for salinity as described in Buck et al. (2007).

Sensitivity determination—The sensitivity (defined as nA nmol L^{-1} s^{-1}) for all samples was determined by internal calibration from the linear portion of the titration curve at the end of the titration, where it is assumed all ligands are saturated with added dFe. The internally calibrated sensitivity was compared with the sensitivity determined by ''overload titration'' (Kogut and Voelker 2001) for BBL samples to ensure an accurate sensitivity due to the high organic matter content and potential presence of HS in BBL samples. Overload titrations, as described by Kogut and Voelker (2001), are an additional method for determining the sensitivity in coastal seawater samples. These titrations are completed at high analytical windows (high $\alpha_{Fe(SA)_2}$) in order to completely outcompete the natural ligands present in the sample. This method also uses an internally calibrated sensitivity but ensures that the ligands are fully titrated by outcompeting them (Kogut and Voelker 2001). This is a concern in coastal samples, because HS have been shown to have measured effects on the sensitivity in cathodic stripping voltammetry analyses using SA (Laglera et al. 2011) and could lower the internal sensitivity. The internal calibrations and overload titrations were also compared with the sensitivity determined in ultraviolet (UV)-irradiated seawater (UVSW, made from UV-irradiating BBL sample at Sta. 10 in the summer 2011) with 22 μg L^{-1} HS subsequently added (Suwannee River fulvic acid (SRFA) standard; SRFA International Humic Substances Society) to determine the effect of HS on the sensitivity determinations (Lagleraet al. 2011). First, 22 μg L^{-1} HS was added to UVSW and titrated with 0, 1, 5, and 10 nmol L^{-1} of added Fe, and the sensitivity was determined from the linear portion of the titration curve, as in the internal sensitivity calculation. Iterative sensitivity determinations have also been used in recent studies to address the issues associated with high organic content samples (Hudson et al. 2003; Wu and Jin 2009), but they may overestimate the sensitivity in some cases (Laglera et al. 2013). In this study, we chose to compare internal calibrations, overload titrations, and UVSW titrations with HS for determining the most accurate sensitivity for the seawater matrix in this coastal region.

Multiple analytical window analysis—dFe speciation samples were analyzed using CLE-ACSV with MAWs of the added competing ligand (SA). The analytical windows employed were determined based on the estimated side reaction coefficients (i.e., carrying capacity) of the ambient ligand pool (α_L) and that of the competing ligand ($\alpha_{Fe(SA)_2}$). When the ratio of these two side reaction coefficients ($\log \alpha_L : \log \alpha_{Fe(SA)_2}$) is between 1 and 10, then the chosen analytical window is appropriate for detecting that ligand class (van den Berg and Donat 1992; Ibisanmi et al. 2011). The side reaction coefficient, α, is determined by

$$\alpha_L = 1 + \sum_{i}^{n} ([L]^n \times K^{cond}_{FeL_n,Fe'}) \quad (1)$$

where [L] is the concentration of the ligand (natural or competing) and $K^{cond}_{FeL_n,Fe'}$ is the conditional stability constant. For SA, the $K^{cond}_{FeL_n,Fe'}$ is noted as $\beta^{cond}_{SA_2,Fe'}$ because SA is thought to form an electroactive bis complex with Fe as experimentally determined by Rue and Bruland (1995) and Buck et al. (2007) at a concentration of 25–27.5 μmol L^{-1} SA ($\alpha_{Fe(SA)_2}$ = 60–75). A separate calibration of SA was completed here for the relevant concentrations of SA (17–32 μmol L^{-1}) and was not found to differ substantially from Buck et al. (2007). The $\beta^{cond}_{SA_2,Fe'}$ determined by the Buck et al. (2007) calibration was therefore used for all determinations of $\alpha_{Fe(SA)_2}$ in this study. This work aimed to detect both strong and weak dFe-binding ligands; thus, a range of detection windows were used in the surface and BBL. The $\alpha_{Fe(SA)_2}$ range of 30–100 was chosen to ensure the competing ligand would still outcompete the strong inorganic side reactions for Fe ($\alpha_{Fe'} = 10$) on the low [SA] end, but not too strong to completely outcompete all natural ligands at the high end (Rue and Bruland 1995). A $\log \alpha_L : \log \alpha_{Fe(SA)_2}$ from 1 to 10 was determined in all titrations except one (ratio equal to 10.15, data not shown), ensuring that the analytical windows chosen were appropriate for the ambient ligand pool present in the samples (van den Berg and Donat 1992; Ibisanmi et al. 2011).

Dissolved HS analyses—Determination of dissolved HS was completed by ACSV analysis as described above for dFe speciation titrations but fine-tuned for HS determination with the modifications described by Laglera et al. (2007). Briefly, boric acid buffer (pH 8.2, NBS) and dFe were added to each 10 mL aliquot of the sample to sufficiently saturate the excess Fe-binding HS (20–50 nmol L^{-1} Fe). Several concentrations (5–300 μg L^{-1}) of SRFA standard (20 mg L^{-1} stock solution) were then added to five of the aliquots, and three aliquots had no added HS. The Fe and HS additions were then equilibrated for at least 2 h. Immediately before analysis, 400 μL of 0.4 mol L^{-1} potassium bromate (> 99%, VWR International) was added as an oxidative catalyst for the reaction, and each aliquot was analyzed as described by Laglera et al. (2007) at a −0.1 V deposition potential, with a 50 mV s^{-1} scan rate in linear sweep mode. The [HS] in the samples was determined by the standard addition method, and the resulting concentrations determined in each sample represent HS that contribute to the observed electrochemical peak at −0.6 V.

dFe speciation data processing—Several advanced numerical methods exist for processing complex ligand data (Hudson et al. 2003; Garnier et al. 2004; Wu and Jin 2009) and one using MAWs (Sander et al. 2011), but to date, none of these methods are publicly available. An intercomparison of data processing methods is currently underway (S. G. Sander unpubl.), but another recent intercomparison effort found reasonable agreement in open ocean samples between the method used here and the Gerringa et al. (1995) nonlinear method (Buck et al. 2012). Recent numerical methods have used only simulated titration data (Garnier et al. 2004; Wu and Jin 2009) or data from estuaries, which likely contain a much larger continuum of binding capacities (Hudson et al. 2003; Sander et al. 2011). Most methods agree in the detection of L_1 ($\log K^{cond}_{FeL,Fe'} \geq 12.0$), although some discrepancy exists in the detection of L_2 due to underestimations of the sensitivity (Wu and Jin 2009; Ibisanmi et al. 2011). Extra care was taken in this study to determine an accurate sensitivity in BBL samples, in which sensitivity underestimation is likely to be a problem. Ligand concentrations and conditional stability constants were determined using averages and standard deviations of both van den Berg–Ružić linearizations (Ružić 1982; van den Berg 1982) and Scatchard linearizations (Scatchard 1949; Mantoura and Riley 1975; Buck et al. 2012). Ligand classes were then characterized simply by their log $K^{cond}_{FeL,Fe'}$ to avoid ambiguity in the literature between ligand classes defined by relative as opposed to absolute binding strengths (Gledhill and Buck 2012). "Stronger" ligands in this study are presented as L_1 ($\log K^{cond}_{FeL,Fe'} \geq 12.0$) and L_2 ($12.0 > \log K^{cond}_{FeL,Fe'} \geq 11.0$), whereas the "weaker" ligand pool is represented as L_3 ($11.0 > \log K^{cond}_{FeL,Fe'} \geq 10.0$) and L_4 ($\log K^{cond}_{FeL,Fe'} \leq 10.0$). These L_1 and L_2 ligand classes represent the pool of stronger dFe-binding ligands in the literature, and our L_3 and L_4 classes represent the weaker ligand pool (Table 1; following the convention of Gledhill and Buck 2012). The distinction between ligand classes is operationally defined by the conditional stability constant values, so the concentration of excess ligand (eL; $[L_x] - [dFe]$) and overall complexing capacity (α_L, or the side reaction coefficient of the sample) were also determined to compare across analytical windows and ligand classes.

Statistical analyses—To examine relationships between all collected variables, Pearson's correlation analysis was used on the data (nonnormalized). To address the ligand data specifically, a contingency table was made of the average ligand concentrations from each season and sampling location (surface and BBL at all analytical windows) based on the presence or absence of each class of ligand during that season. A ligand class was considered to be present if it was measured in at least one sample ($n \geq 1$, Table 2) and considered not present if it was not measured ("nd," or not detected, in Table 2). Statistical differences in the presence or absence of ligands between seasons and sampling locations (surface and BBL) were then assessed in this contingency table using chi-square analysis. Multivariate statistical analyses were used to compare associations between physical and chemical

Table 2. Average ligand (L_1, L_2, L_3, L_4) concentrations and conditional stability constants ($\log K_1$, $\log K_2$, $\log K_3$, $\log K_4$) for each analytical window ($\alpha_{Fe(SA)_2}$) during the May 2010 (spring) and August and September 2011 (summer) sampling periods. Averages and standard deviations are shown for surface and benthic boundary layer samples from each season, where n represents the number of titrations. Ligand concentrations are also shown from "overload" titrations in the spring samples ($\alpha_{Fe(SA)_2} = 500, 251$). nd, a parameter for which there is no data.

Season	Location	α	n	$[L_1]$	+/−	$\log K_1$	+/−	n	$[L_2]$	+/−	$\log K_2$	+/−	n	$[L_3]$	+/−	$\log K_3$	+/−	n	$[L_4]$	+/−	$\log K_4$	+/−	$\log \alpha_L$	+/−
Spring 2010	Surface	100	6	5.2	2.9	12.1	0.1	7	4.4	1.6	11.6	0.3	1	2.0	nd	10.9	nd	0	nd	nd	nd	nd	14.5	0.4
		60	8	3.4	1.9	12.2	0.2	16	4.2	3.2	11.5	0.2	3	3.3	1.6	10.6	0.3	0	nd	nd	nd	nd	14.2	0.4
		30	3	4.1	1.0	12.1	0.2	5	2.6	1.2	11.6	0.3	10	4.6	2.9	10.7	0.4	0	nd	nd	nd	nd	14.1	0.5
	BBL	500	1	12.9	nd	12.2	nd	0	nd	nd	nd	nd	0	nd	nd	nd	nd	0	nd	nd	nd	nd	15.3	nd
		251	3	10.1	5.1	12.4	0.5	2	11.9	4.4	11.9	0.0	0	nd	nd	nd	nd	0	nd	nd	nd	nd	15.2	0.5
		100	3	16.2	1.1	12.2	0.2	10	15.2	4.8	11.4	0.3	0	nd	nd	nd	nd	0	nd	nd	nd	nd	14.8	0.5
		60	0	nd	nd	nd	nd	8	15.8	4.4	11.3	0.2	5	15.0	5.7	10.8	0.1	1	14.0	nd	10.0	nd	14.4	0.4
		30	0	nd	nd	nd	nd	7	14.4	3.4	11.2	0.3	4	17.0	7.4	10.7	0.2	0	nd	nd	nd	nd	14.2	0.3
Summer 2011	Surface	100	13	4.4	2.7	12.3	0.3	15	4.3	2.2	11.6	0.3	3	6.0	2.8	11.0	0.2	1	21.8	nd	9.7	nd	14.4	0.5
		60	10	3.6	1.9	12.3	0.3	17	3.6	1.8	11.4	0.3	11	4.5	1.8	10.6	0.3	3	13.9	13.6	9.8	0.1	14.1	0.6
		30	3	4.0	3.2	12.2	0.0	13	3.8	2.1	11.4	0.3	13	5.0	2.4	10.7	0.3	3	68.8	66.1	9.3	0.8	13.6	0.6
	BBL	100	4	13.6	9.6	12.2	0.1	12	11.4	5.5	11.5	0.3	2	24.5	16.3	10.7	0.4	0	nd	nd	nd	nd	14.7	0.5
		60	2	7.2	2.5	12.1	0.0	11	12.9	7.4	11.5	0.2	5	19.6	7.8	10.4	0.2	0	nd	nd	nd	nd	14.4	0.5
		30	0	nd	nd	nd	nd	7	10.0	3.8	11.5	0.3	6	15.2	14.2	10.5	0.2	4	21.3	15.9	9.8	0.1	13.8	0.7

parameters. A standard principal component analysis (PCA) was used to reduce the dimensionality (number of variables) of the dataset and investigate interactions between the measured variables. For the PCA, the dataset was first scaled by the standard deviation of each variable to weight equally the contribution of each variable to the dataset. PCA was then performed on the data matrix comprising 18 variables (latitude, longitude, depth, temperature, salinity, nitrate, phosphate, silicate, [dFe], [L_1], log K_1, [L_2], log K_2, [L_3], log K_3, [L_4], log K_4, and distance from shore) and 82 samples. Missing values in the dataset were filled using the average value for that variable at that depth and season, except for the ligand concentrations, which were noted as zero if they were not detected. For example, a missing surface nutrient data point was filled with the average concentration that was determined in the surface during that season from the current dataset. There were anywhere from 0 to 12 missing values for a given variable within the dataset. If more than 12 data points were missing, then the variable was excluded from the statistical analyses (i.e., Chl *a*). All statistics were deemed significant at $p < 0.05$ and were calculated using the Matlab statistics and bioinformatics toolbox.

Results

Hydrography and dFe distributions—In-depth dFe and hydrographic results are reported elsewhere (Biller et al. 2013). Temperature, salinity, Chl *a*, and nutrient concentrations for all stations sampled for dFe speciation are presented in Table 3. Macronutrient, Chl *a*, and dFe data for the remaining stations can be found in Biller et al. (2013); only a subset of that data is presented here. Surface samples taken during the spring cruise had lower average temperatures (10.4 ± 1.5°C, $n = 20$) and higher average macronutrient concentrations (17.1 ± 10.1 μmol L^{-1} NO_3^-, 1.3 ± 0.6 μmol L^{-1} PO_4^{3-}, and 25.4 ± 14.9 μmol L^{-1} $Si(OH)_4$, $n = 20$) than those sampled during the summer cruise (12.5 ± 1.8°C, 13.5 ± 8.0 μmol L^{-1} NO_3^-, 1.3 ± 0.6 μmol L^{-1} PO_4^{3-}, and 17.9 ± 14.9 μmol L^{-1} $Si(OH)_4$, $n = 33$), likely due to intense upwelling conditions during the spring cruise (Fig. 1 and National Oceanic and Atmospheric Association upwelling index http://www.pfeg.noaa.gov/products/las.html, data not shown). Surface samples in the spring also contained relatively higher Chl *a* concentrations, with 5.9 ± 9.2 μg L^{-1} ($n = 20$) on average in the surface waters sampled for dFe speciation compared with the summer (3.5 ± 3.6, $n = 33$). Chl *a* concentrations were not determined in the BBL samples. BBL conditions were similar during both cruises, with similar average NO_3^- (29.8 ± 1.1, $n = 12$ and 30.0 ± 3.7 μmol L^{-1} NO_3^-, $n = 17$) and temperatures (8.3 ± 0.3, $n = 12$ and 9.4 ± 1.0°C, $n = 17$) in the spring and summer, respectively. The PO_4^{3-} and $Si(OH)_4$ concentrations were similar for BBL samples during the spring and summer cruise, but BBL samples on average contained higher concentrations of both PO_4^{3-} (2.3 ± 0.1 μmol L^{-1}, $n = 12$; 2.6 ± 0.3 μmol L^{-1}, $n = 17$) and $Si(OH)_4$ (47.6 ± 3.4 μmol L^{-1}, $n = 12$; 44.7 ± 10.0 μmol L^{-1}, $n = 17$) relative to surface samples in the spring and summer, respectively.

The highest NO_3^- concentrations measured in the surface waters during both cruises were observed north of San Francisco Bay off Point Reyes, Point Arena, and Cape Mendocino (Fig. 2C,D). This region generally correlated with higher Chl *a* concentrations as observed from satellite (Fig. 1C,D; CoastWatch Aqua Moderate Resolution Imaging Spectroradiometer), and from underway measurements (Table 3). These areas also corresponded to the some of the highest [dFe] (Fig. 2A,B) and lowest temperatures (Fig. 1, Table 3) observed. Higher [dFe] were measured on average in the surface during the spring (Biller et al. 2013). Similar [dFe] were found between seasons in the BBL, with higher concentrations observed in some repeat sampling locations in the spring and vice versa in the summer (Biller et al. 2013). In the BBL, the highest dFe and NO_3^- concentrations were also observed north of San Francisco Bay (Fig. 3) during both cruises. Relatively lower [dFe] and NO_3^- were observed south of Monterey Bay, along the narrow Big Sur coastline (Wheatcroft et al. 1997), also corresponding to lower average Chl *a* concentrations (Fig. 1C,D).

Sensitivity determinations for ACSV measurements—The sensitivities (nA nmol L^{-1} s^{-1}) in all surface samples were determined by internal calibration (Rue and Bruland 1995) from the linear portion of the titration curve, where it is assumed that all ligands have been titrated by the excess dFe additions. Internally measured sensitivities in BBL samples were then compared with two other methods to ensure accurate determination of the sensitivity. An $\alpha_{Fe(SA)_2}$ of 251 and 500 were employed in "overload" titrations (Kogut and Voelker 2001; Table 2), and these $\alpha_{Fe(SA)_2}$ were estimated to be outside the analytical window for the ligand pool in the BBL based on the ratio of log α_L : log $\alpha_{Fe(SA)_2}$. The sensitivities determined by overload titration were less than the average sensitivity determined by internal calibration at all analytical windows employed in the sample analyses, but the differences were not statistically significant ($\alpha_{Fe(SA)_2}$ of 30, 60, and 100; *t*-test, $t = 0.16$, degrees of freedom (df) = 28, $p > 0.05$). The average sensitivity determined by internal calibration at $\alpha_{Fe(SA)_2} = 30$, 60, and 100 was 1.27 ± 0.88 ($n = 29$), 1.28 ± 0.80 ($n = 45$), and 0.82 ± 0.39 ($n = 28$), respectively. Using $\alpha_{Fe(SA)_2} = 500$ ($n = 1$), the sensitivity determined by overload titration was 0.21 nA nmol L^{-1} s^{-1}, and with $\alpha_{Fe(SA)_2} = 251$ ($n = 4$), the sensitivity was 0.66 ± 0.20 nA nmol L^{-1} s^{-1}. These differences in sensitivity, with a lower average sensitivity at higher analytical windows, included considerable variability and were not significant ($p > 0.05$).

With no statistical differences observed between internal and overload sensitivities, additional sensitivity tests were performed using UVSW (a UV-irradiated sample from BBL Sta. 10 in the summer) with added HS (22 μg L^{-1}) to confirm the validity of internal calibration in the presence of HS in BBL samples, since high variability was observed. Sensitivities determined at each analytical window using UVSW and added HS were also found to be statistically indistinct from those internally calibrated in the BBL sample analyses (*t*-test; $t = 0.29$, 0.27, 0.96; df = 28, 44, 27; $p = 0.78$, 0.79, and 0.36 for $\alpha_{Fe(SA)_2} = 100$, 60, and 30, respectively).

dFe-binding ligand distributions in surface waters—Averaged dFe speciation results of all samples at each analytical window are presented in Table 2. Although the average ligand concentrations and conditional stability constants are presented for every analytical window, the detection of each ligand class was found to be optimal at specific windows based on the ratio of log α_L : log $\alpha_{Fe(SA)_2}$. Therefore, the distributions of each ligand class are only presented at their optimized window ($\alpha_{Fe(SA)_2} = 100$ for L_1, 60 for L_2, and 30 for L_3 and L_4; Figs. 4, 5)

Similar concentrations and strengths of ligands were observed in the spring and summer in the surface waters. Chi-square analysis based on a contingency table of the ligand data revealed there was no significant difference between the ligands observed in the spring and the summer ($p > 0.05$). Figure 4 presents the distribution of average concentrations of each ligand class across both seasons in the study area.

Stronger ligand pool (L_1 and L_2): Spatial distributions of the stronger ligand classes in surface waters are shown together for both cruises in Fig. 4A,B, with L_1 presented from the highest analytical window ($\alpha_{Fe(SA)_2} = 100$) and L_2 presented from the middle analytical window ($\alpha_{Fe(SA)_2} = 60$). Stronger ligand concentrations were generally highest closest to shore and decreased offshore. Excess ligand concentrations ([L_x] − [dFe], eL) also followed this trend (data not shown). Elevated concentrations of strong dFe-binding ligands were observed just outside the mouth of San Francisco Bay (4.8 and 7.5 nmol L^{-1}), near Point Reyes (10.2 nmol L^{-1}), and south of Cape Mendocino (7.3 nmol L^{-1}). These ligand concentrations were among the highest observed in surface waters. The strongest ligands (L_1) were not observed in any of the offshore stations (Fig. 4A), although L_2 ligands were detected at almost all stations and in fact were the most common ligand class detected in surface waters. The complexation capacity generally decreased offshore as the concentrations of the strongest ligands declined (Table 2). Although the observations were patchy between cruises, in general the highest concentrations and strongest ligands were found closest to shore in the northern part of the study region and near the mouth of San Francisco Bay.

Weaker ligand pool (L_3 and L_4): The highest concentrations of weaker ligands (L_3 and L_4) in surface waters were measured at the lowest analytical window ($\alpha_{Fe(SA)_2} = 30$), the window optimized for weaker ligand detection. The average concentrations of L_3 ligands were similar between the spring and summer (4.6 ± 2.9 nmol L^{-1}, $n = 10$ in spring and 5.0 ± 2.4 nmol L^{-1}, $n = 13$ in summer; Table 2), and chi-square analysis based on the frequency of L_3 detections in both seasons showed there was no significant difference between the two seasons ($p > 0.05$). The L_3 ligands in the weaker ligand pool showed a distinct spatial distribution (Fig. 4C) compared with the stronger ligand pool (L_1 and L_2; Fig. 4A,B). While the stronger ligands generally declined offshore, higher concentrations of L_3 ligands were detected in the furthest offshore stations. The L_4 ligands, or the weakest ligands in the observed ligand pool, were not detected at all in surface waters during the spring, and only three surface samples contained L_4 ligands during the summer cruise (Table 2). Their concentrations were highly variable (ranging from 6 to 140 nmol L^{-1}), and were only found in two stations near the mouth of San Francisco Bay (Fig. 1B), and north of Cape Mendocino (Figs. 1, 4D). No L_4 ligands were detected in surface waters offshore from the continental shelf.

dFe-binding ligand distributions in the BBL—Stronger ligand pool (L_1 and L_2): The strongest ligands (L_1) were only detected at the two highest analytical windows ($\alpha_{Fe(SA)_2} = 100, 60$) in the BBL and were detected less frequently in the BBL compared with the surface waters. The concentrations of L_1 were higher in spring (16.2 ± 1.1 nmol L^{-1}, $n = 3$; Table 2) than in the summer (13.6 ± 9.6 nmol L^{-1}, $n = 4$ at $\alpha_{Fe(SA)_2} = 100$ and 7.2 ± 2.5 nmol L^{-1}, $n = 2$ at $\alpha_{Fe(SA)_2} = 60$; Table 2), although not significantly so (chi-square, $p > 0.05$). The strongest ligands were not detected in all BBL samples, and were found most frequently in samples surrounding San Francisco Bay and Point Arena (Fig. 5, $\alpha_{Fe(SA)_2} = 100$). The L_2 ligands were detected much more frequently in the BBL compared with L_1 ligands ($n = 9$ in spring and summer for L_1 vs. $n = 55$ for L_2) and were found at every analytical window during both seasons (Table 2). In general, higher concentrations of L_2 ligands were measured in the spring than in the summer, but not significantly so (chi-square, $p > 0.05$). The concentrations of L_2 ligands were highest in the areas with the highest [dFe] in the BBL (Fig. 5; $\alpha_{Fe(SA)_2} = 60$) but were present in all of the sampling regions. Relatively high concentrations of stronger ligands in the BBL lead to higher complexation capacities in these samples than in surface waters (Table 2).

Weaker ligand pool (L_3 and L_4): While weaker ligands were most commonly detected at the lower analytical windows during the spring and summer within the BBL (Table 2), two samples had detectable L_3 ligands at even the highest analytical window. High variability was seen during both seasons in the concentrations of L_3 and L_4 ligands in the BBL (standard deviations up to 67%; Table 2). The L_3 ligand class was detected in BBL samples from all regions of the study area, including the shelf areas outside of San Francisco Bay, Point Arena, Cape Mendocino, and Big Sur (Fig. 5; $\alpha_{Fe(SA)_2} = 30$). Higher [L_3] generally coincided with higher [dFe], and [L_3] was always in excess of [dFe]. The L_4 ligand class showed a distinct distribution compared with all the other ligand classes. L_4 ligands were only detected in five samples in the BBL (Table 2), and all of these samples were within the San Francisco Bay region or the Cape Mendocino region (Fig. 5; $\alpha_{Fe(SA)_2} = 30$). The [L_4] were within the range observed for L_3 ligands in the BBL (14–21 nmol L^{-1}) and showed similar variability (50–70% standard deviation), but were detected less frequently in BBL samples.

Dissolved HS—Dissolved HS were measured in two BBL samples during the summer cruise in 2011 at Stas. 10 and 37 (Sta. 10: 40.767°N, 124.386°W; Sta. 37: 37.418°N, 122.611°W) to determine the influence of HS on the Fe-binding ligand pool in the BBL. Station 10 was located on the continental shelf near Cape Mendocino at 64 m depth,

Table 3. Hydrographic (temperature [T] and salinity), Chl *a*, and macronutrient (nitrate [= nitrite + nitrate], phosphate, silicate) data for all stations (Sta.) sampled for organic Fe-binding ligands during May 2010 and August and September 2011 in the surface and benthic boundary layer. nd, a parameter for which there is no data.

Date sampled	Transect	Sta.	Latitude (°N)	Longitude (°W)	Depth (m)	T (°C)	Salinity	Chl *a* (μg L^{-1})	Nitrate (μmol L^{-1})	Phosphate (μ mol L^{-1})	Silicate (μmol L^{-1})
May 2010	1	2	39.1830	−123.8267	2	9.34	33.38	1.27	27.4	2.0	43.5
		3	39.4512	−123.8869	2	9.71	33.56	0.00	24.7	1.8	33.9
		4	39.7025	−123.8817	2	11.18	33.33	0.00	25.4	1.9	34.6
		5	39.9421	−124.0867	2	9.82	34.01	0.00	29.6	2.2	44.8
		6	40.1510	−124.3092	2	15.57	35.48	0.00	29.9	2.2	51.2
		7	40.3781	−124.5318	2	11.29	33.00	0.00	13.9	1.2	24.4
	2	1	40.1917	−125.1827	2	12.22	32.28	0.00	0.0	0.3	3.7
		2	39.8687	−124.9036	2	11.71	32.11	1.92	1.0	0.3	5.0
		3	38.9608	−124.4121	2	10.26	32.69	1.99	19.0	1.4	26.8
	6	1	38.2712	−123.1036	2	8.58	33.99	1.01	29.3	2.1	41.4
		2	38.5350	−123.8423	2	9.72	33.33	0.37	21.1	1.5	25.1
		3	38.5747	−123.9531	2	10.27	33.36	6.86	12.1	1.0	13.6
	8	1	38.7817	−124.4115	2	10.83	32.28	14.01	5.1	0.6	8.2
		2	38.9321	−123.9908	2	11.36	32.27	3.58	2.3	0.5	2.3
		3	39.0100	−123.7887	2	9.92	32.54	1.36	21.5	1.6	30.1
		4	39.3341	−123.8415	2	9.18	33.94	30.69	17.2	1.2	28.5
	9	1	39.5342	−123.8333	2	9.11	33.12	14.86	21.0	1.4	30.4
		2	39.6638	−124.0785	2	9.35	33.04	12.65	16.6	1.3	22.8
		3	39.8516	−123.9394	2	9.49	33.11	28.74	6.3	0.6	13.4
		4	39.9199	−124.2714	2	10.63	33.27	4.07	7.1	0.9	8.0
	10	1	38.6430	−123.4439	2	9.03	33.89	0.17	28.5	2.1	41.9
	11	1	37.9411	−122.9649	58	8.28	34.03	nd	29.3	2.2	49.5
		2	37.9063	−122.8802	53	8.50	34.01	nd	28.8	2.1	45.3
		3	37.7817	−122.9515	62	8.37	34.03	nd	29.4	2.2	42.9
		4	37.8706	−123.0930	86	8.61	33.98	nd	28.6	2.1	41.2
		5	38.1120	−123.1234	74	8.19	34.04	nd	29.6	2.2	48.3
		6	38.1108	−123.0256	61	8.37	34.01	nd	28.8	2.2	43.9
		7	38.2553	−123.0805	69	8.14	34.04	nd	29.6	2.3	50.8
		8	38.4600	−123.2448	67	8.06	34.04	nd	29.1	2.2	51.2
		9	38.6386	−123.4310	69	7.78	34.05	nd	30.0	2.3	51.2
		10	38.7849	−123.6212	65	7.80	34.05	nd	30.4	2.3	50.3
		17	39.0301	−123.7690	68	7.77	34.05	nd	31.9	2.4	49.5
		19	39.3341	−123.8415	78	7.87	34.03	nd	31.9	2.4	46.4
		23	38.6390	−123.4369	72	8.02	34.04	nd	29.7	2.4	48.7
Aug 2011	1	1	38.0233	−123.0889	2	11.81	33.65	5.86	18.1	1.7	27.9
		2	38.2004	−123.1060	2	12.06	33.61	1.76	17.5	1.8	24.5
		3	38.6353	−123.4926	2	10.75	33.82	0.08	26.8	2.3	33.6
		4	38.9050	−123.7876	2	11.40	33.49	2.41	17.2	1.4	19.8
		5	39.3911	−123.8968	2	10.81	33.53	10.13	15.7	1.3	13.1
	2	1	39.7127	−124.6647	2	16.09	32.66	0.08	0.0	0.3	2.8
		2	39.1683	−124.2509	2	11.83	32.89	0.00	6.8	0.8	8.2
	5	1	37.7793	−126.2642	2	17.16	33.15	0.00	3.8	0.6	2.5
		2	38.0066	−125.7003	2	15.26	33.14	0.00	5.4	0.6	3.8
		3	38.0181	−124.9463	2	13.31	33.38	3.09	nd	nd	nd
	7	1	38.0684	−124.4368	2	14.51	33.18	0.14	6.6	0.7	5.5
		2	38.2556	−124.1933	2	13.25	33.31	1.30	11.7	1.0	9.8

Table 3. Continued.

Date sampled	Transect	Sta.	Latitude (°N)	Longitude (°W)	Depth (m)	T (°C)	Salinity	Chl *a* (μg L^{-1})	Nitrate (μmol L^{-1})	Phosphate (μ mol L^{-1})	Silicate (μmol L^{-1})
		3	38.3498	−124.0705	2	12.42	32.89	1.50	5.3	nd	7.1
		4	38.6132	−123.7229	2	12.39	32.86	1.18	7.4	0.8	8.0
	17	2	38.7832	−123.6176	2	10.38	33.70	3.18	25.5	2.1	32.5
		3	38.8247	−123.6500	2	10.08	33.76	1.56	25.5	2.1	34.2
		4	38.8183	−123.6602	2	10.13	33.75	1.96	25.0	2.1	33.8
		5	38.7998	−123.6887	2	10.92	33.52	3.96	19.0	1.6	23.0
		6	39.1725	−123.7926	2	10.86	33.74	2.56	22.5	1.8	33.3
		7	39.3333	−123.8426	2	10.44	33.85	2.35	26.6	2.2	39.6
		8	39.5356	−123.8295	2	11.42	33.62	9.81	0.5	0.4	5.9
		9	40.7374	−124.3291	2	11.64	33.62	4.05	13.5	1.0	13.3
		10	40.7672	−124.3858	2	10.81	33.57	2.84	18.6	1.4	19.2
		11	40.7885	−124.4169	2	11.94	33.38	1.31	16.6	1.3	16.6
		12	40.8169	−124.4664	2	12.93	33.38	1.45	13.4	1.0	12.6
		23	37.2802	−122.5273	2	13.54	33.54	15.95	0.2	0.3	1.7
		31	35.6452	−121.3041	2	12.18	33.58	7.21	10.5	0.9	7.7
		33	36.0606	−121.6140	2	12.27	33.52	nd	15.6	1.5	17.6
		35	36.2169	−121.8065	2	11.71	33.65	6.95	14.5	1.3	15.9
		37	37.4180	−122.6109	2	14.45	33.36	6.62	3.3	0.4	8.7
		38	37.6034	−122.8299	2	12.88	33.28	nd	10.5	1.2	21.7
		39	37.7583	−123.0007	2	13.17	33.31	nd	8.8	0.9	14.8
		2	38.7832	−123.6176	64	9.18	33.94	nd	31.1	2.8	51.9
		3	38.8247	−123.6500	48	9.18	33.94	nd	31.8	2.9	50.5
		4	38.8183	−123.6602	61	9.12	33.95	nd	31.4	2.8	52.8
		5	38.7998	−123.6887	90	9.04	33.96	nd	31.2	2.6	48.6
		6	39.1725	−123.7926	70	9.34	33.92	nd	31.3	2.6	50.3
		7	39.3333	−123.8426	81	9.17	33.94	nd	31.6	2.7	49.6
		8	39.5356	−123.8295	68	9.13	33.94	nd	31.4	2.6	47.8
		9	40.7374	−124.3291	40.3	8.72	33.90	nd	30.5	2.7	47.2
		10	40.7672	−124.3858	64	8.60	33.93	nd	30.5	2.6	45.4
		11	40.7885	−124.4169	100	8.36	34.00	nd	31.8	2.6	46.1
		12	40.8169	−124.4664	339	6.95	34.12	nd	37.2	2.9	60.6
		23	37.2802	−122.5273	75	9.98	33.86	nd	27.5	2.3	36.8
		31	35.6452	−121.3041	56	11.60	33.61	nd	22.1	1.8	23.3
		33	36.0606	−121.6140	49	10.61	33.72	nd	21.4	1.9	24.7
		35	36.2169	−121.8065	79	10.11	33.78	nd	25.9	2.2	28.6
		37	37.4180	−122.6109	64	9.95	33.86	nd	31.0	2.7	48.0
		38	37.6034	−122.8299	67	9.88	33.87	nd	30.9	2.8	49.9
		39	37.7583	−123.0007	62	9.90	33.84	nd	30.9	2.6	42.5
Sep 2011	16	1	37.8264	−122.4663	2	15.62	30.88	3.96	17.8	2.4	42.1
		2	37.7722	−122.5769	2	14.65	31.92	5.55	13.7	1.6	29.6

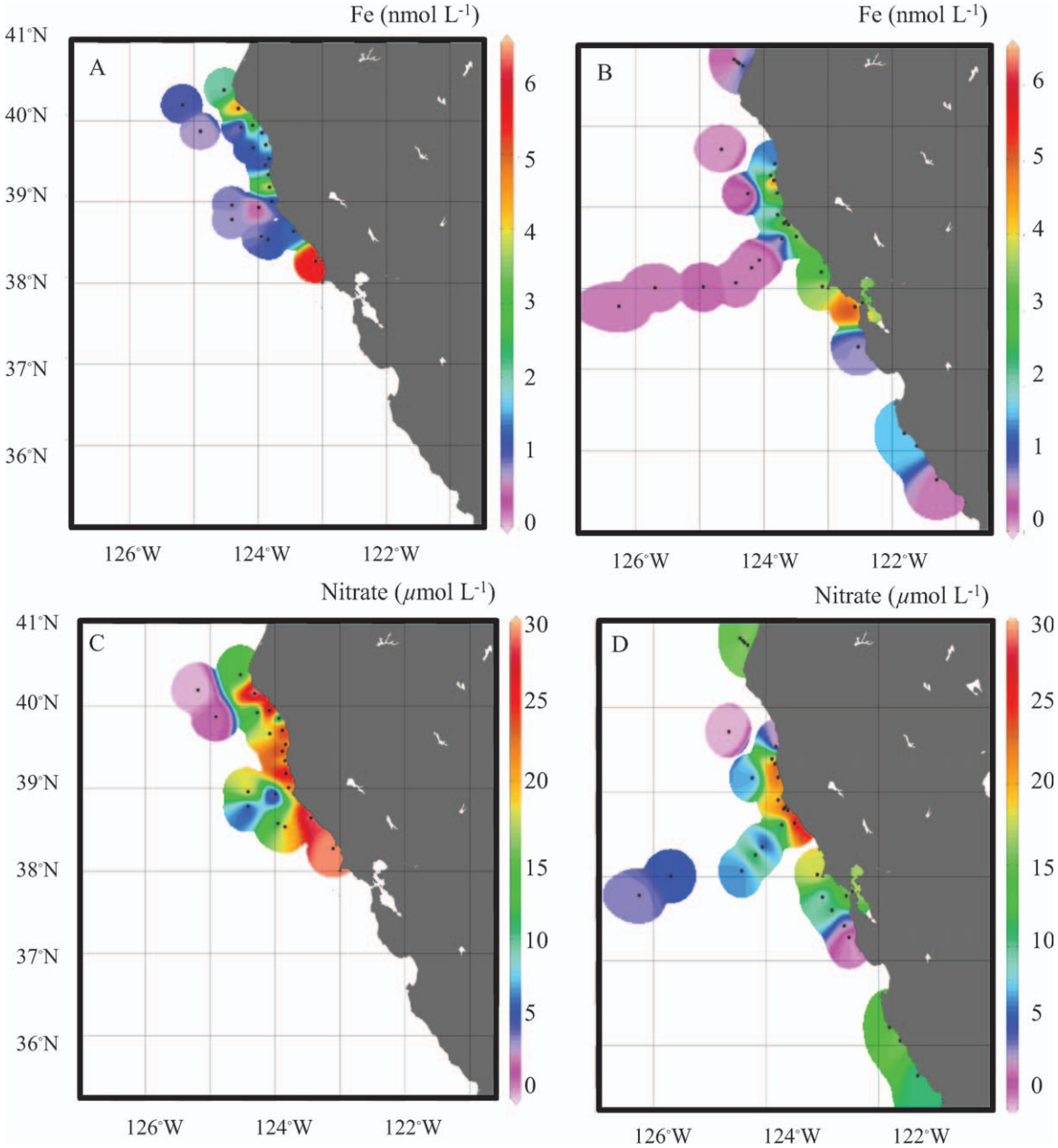

Fig. 2. Surface-dissolved Fe concentrations in the (A) spring and (B) summer at stations with accompanying Fe–organic speciation data. Surface nitrate (nitrate + nitrite) concentrations are also shown in the (C) spring and (D) summer for each station.

and Sta. 37 was sampled just south of San Francisco Bay at the same depth. Station 10 contained higher concentrations of dFe (20.5 ± 0.3 nmol L^{-1}) than Sta. 37 (6.8 ± 0.1 nmol L^{-1}), but less HS. There was 22.6 μg L^{-1} HS measured at Sta. 10, and 39.2 μg L^{-1} HS at Sta. 37 outside of San Francisco Bay. The concentration of HS was related to the Fe complexation by assuming all the measured HS was complexed to dFe. Previous researchers have shown that HS can bind approximately 32 nmol L^{-1} Fe per 1 mg of HS (Laglera and van den Berg 2009), although this can be variable depending on the type and batch of HS (Laglera and van den Berg 2009). Using the approximation of 32 nmol L^{-1} Fe : 1 mg HS, approximately 3.5% of the dFe at Sta. 10 can be bound by HS and 18.5% at Sta. 37 outside of San Francisco Bay. This would also amount to 4.3% and 11.1% of the total ligand pool (only L_2 was detected in these samples), respectively.

Statistical analyses—Pearson's correlation analysis revealed that very few of the ligand parameters correlated linearly with any other variable examined in the dataset (data not shown). To examine these relationships further, several additional statistical techniques were examined. No significant differences in ligands were found between seasons based on chi-square analysis, but there was a significant difference between the presence of ligands in the

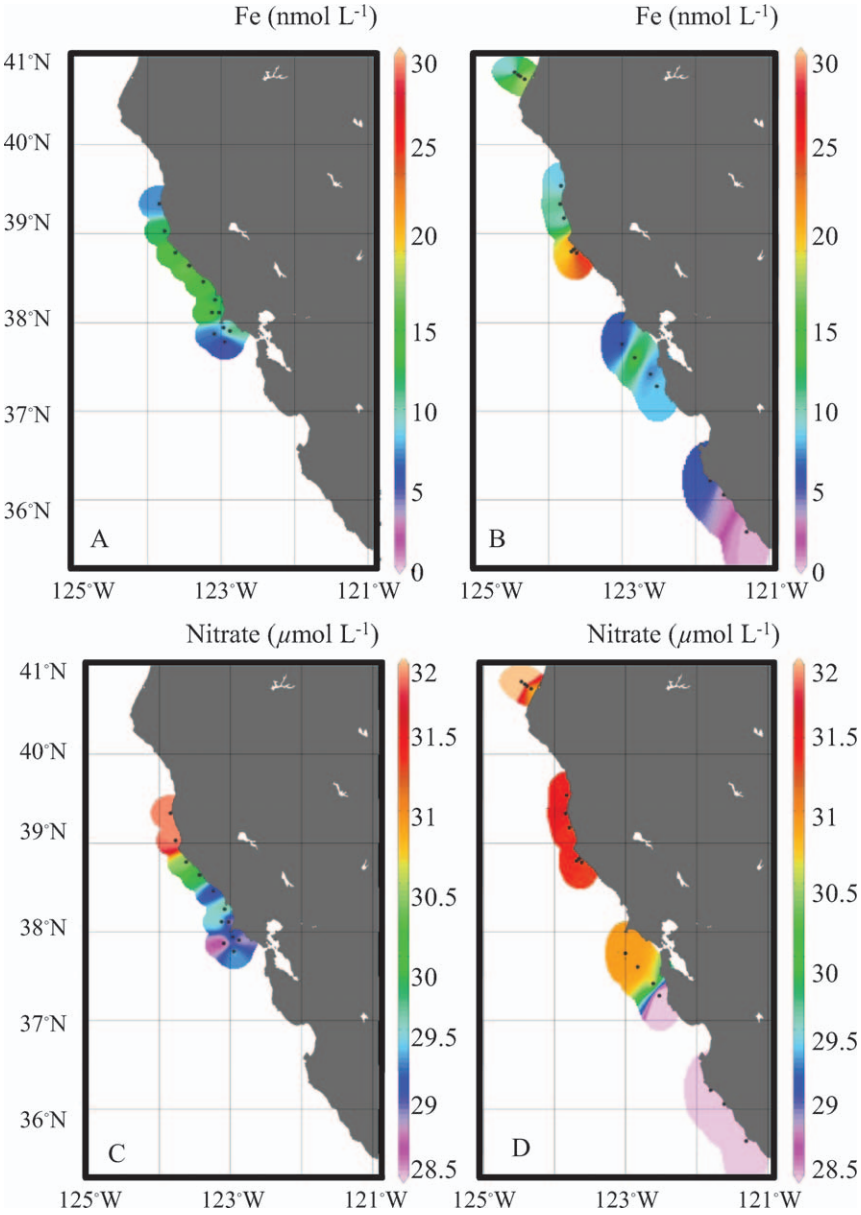

Fig. 3. Dissolved Fe concentrations sampled in the benthic boundary layer (BBL) during (A) spring and (B) summer at stations with accompanying Fe–organic speciation data. BBL nitrate (nitrate + nitrite) concentrations are also shown in the (C) spring and (D) summer for each station.

surface and BBL based on the contingency table (chi-square, $p < 0.025$). PCA was applied to quantify the differences seen between samples in the chi-square analysis. The 18 variables used in the PCA are shown in Table 4, along with their principal component (PC) loadings (eigenvectors) for the first three PCs (Table 4). The PCs are linear combinations of the variables that explain the greatest variance in the dataset (with the first PC explaining the most variance). The first three PCs explained 57% of the variance in the dataset, and the first two explained 46% (data not shown). The first PC was dominated by loadings from temperature, [dFe], NO_3^-, PO_4^{3-}, and $Si(OH)_4$, as can be seen by the magnitude of their eigenvectors (suggesting greater influence on the first PC) in Table 4 and also their distance to the right or left of the vertical "0" axes in Fig. 6A. The variables depth, distance from shore, and salinity contributed to the first PC as well, but to a lesser extent (Fig. 6A). In the first PC, the temperature and distance from shore were inversely related to the [dFe], nutrients, and salinity. The second PC consisted of strong loadings from several of the ligand parameters. The strongest loadings were from L_1, log K_1, L_4, and log K_4 and inversely related to these, but also with strong loadings were L_3, log K_3, and latitude. The contribution of L_2, log K_2, and longitude were similar in magnitude for each PC but opposite in sign, with all three variables showing positive loadings for the second component and negative loadings for the first PC. The third PC was similar to the

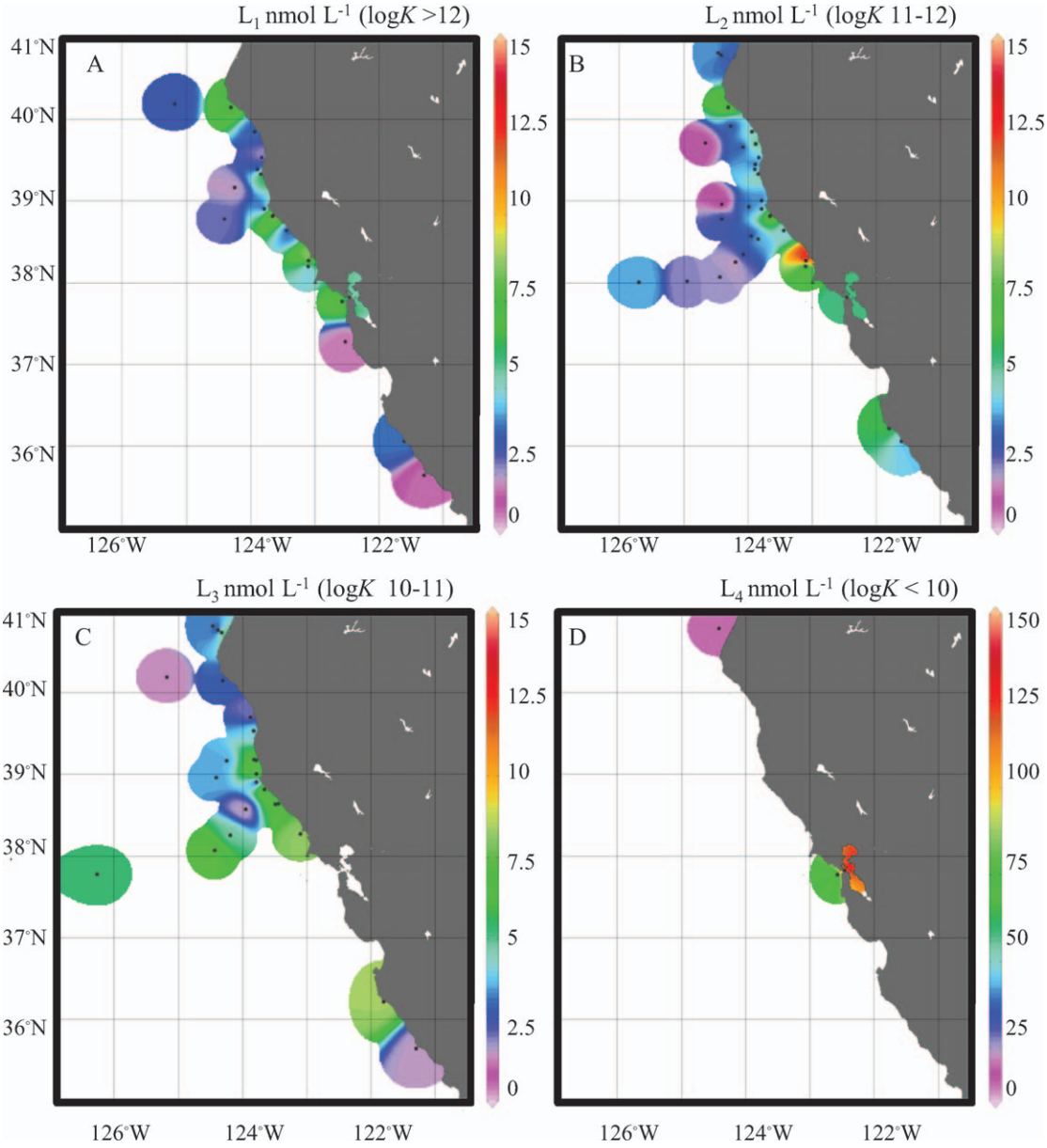

Fig. 4. Ligand concentrations determined in both spring and summer surface waters. (A) The strongest ligands (L_1) measured at $\alpha_{Fe(SA)_2} = 100$; (B) L_2 ligand concentrations measured at $\alpha_{Fe(SA)_2} = 60$, (C) L_3 concentrations at $\alpha_{Fe(SA)_2} = 30$, and (D) L_4 concentrations measured at $\alpha_{Fe(SA)_2} = 30$.

second, but had strong loadings from latitude that were negatively correlated with L_3 and log K_3, as well as longitude and L_1 and log K_1 (Fig. 6B).

When all of the data (surface and BBL, $n = 82$) are plotted in the PC space, there is a clear grouping of surface and BBL samples (Fig. 6C,D). Surface samples group along the positive axis of the first PC, where the variance is strongly related to temperature and distance from shore (Fig. 6C). BBL samples group more along the second PC in the lower left quadrant, where the variance is related to depth, salinity, nutrients (macronutrients and dFe), and L_3 (Fig. 6C). The addition of the third PC does not change the position of the surface samples in the PC space but does shift more of the BBL samples to the upper left quadrant. The variances of samples in this quadrant are also explained by L_2 and log K_2, in addition to those variables strongly related to the second PC.

Discussion

Multiple analytical window analysis—Current electrochemical methodology in detecting dFe-binding ligands constrains the analyst to measuring only one (or sometimes two) ligand classes. This study expands the scope of current electrochemical methods (CLE-ACSV) for detecting a wide range of dFe-binding ligands in seawater. Of the few studies that have used MAW in CLE-ACSV, all have focused on Cu speciation in estuaries (Moffett et al. 1997; Buck and Bruland 2005; Ndung'u 2012), coastal environments (Bundy et al. 2013) or using numerical modeling

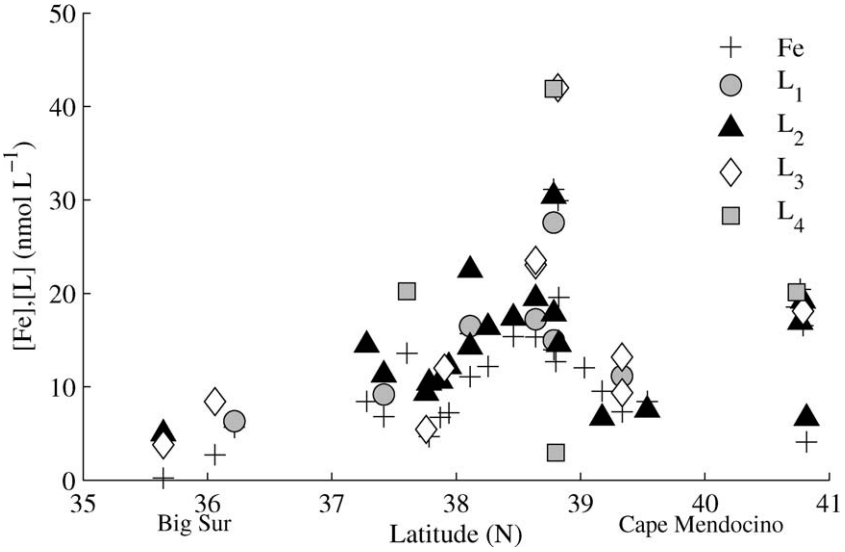

Fig. 5. Dissolved Fe and benthic boundary layer (BBL) ligand concentrations (L_1, L_2, L_3, and L_4) measured in both the spring and summer.

(Sander et al. 2011). This study has extended MAW analysis to dFe speciation. Although a smaller range of ligands is generally thought to be present in seawater for Fe than for Cu (due to the propensity of Fe in seawater to form insoluble (oxy)hydroxides; Liu and Millero 2002), the detection of both weaker and stronger ligands gives insight into the quality of the ligand pool in the surface and BBL in this study. MAW analysis enabled the detection of ligands with a wide range of conditional stability constants (log $K^{cond}_{FeL,Fe'}$ ranging from 9 to 13), similar to the use of MAWs in Cu organic speciation analysis (Bruland et al. 2000), though an even larger range of ligand strengths may be possible as a relatively narrow range in MAWs was employed here.

Table 4. Eigenvectors for the first three principal components (PCs) for each of the variables used in the principal component analysis. The first three PCs explain 57% of the variance. Larger magnitude numbers indicate a stronger contribution to that PC, with positive and negative numbers contributing positively and negatively to that PC, respectively.

Variables	PC1	PC2	PC3
Latitude	0.0084	−0.2053	0.4581
Longitude	−0.1578	0.2290	−0.4632
Depth (m)	−0.2743	−0.1017	0.1394
Temperature (°C)	0.3196	0.1823	−0.0450
Salinity (psu)	−0.2773	−0.2415	−0.0894
Nitrate (μmol L^{-1})	−0.3855	−0.0812	0.0178
Phosphate (μmol L^{-1})	−0.3900	−0.0021	0.0222
Silicate (μmol L^{-1})	−0.3846	−0.0196	0.0701
dFe (nmol L^{-1})	−0.3266	0.0328	0.0791
L_1 (nmol L^{-1})	−0.1571	0.3693	−0.0988
Log K_1	−0.0169	0.3878	−0.2708
L_2 (nmol L^{-1})	−0.2587	0.1738	0.1421
Log K_2	−0.0541	0.1276	0.1969
L_3 (nmol L^{-1})	−0.1053	−0.2424	−0.3381
Log K_3	0.0340	−0.2340	−0.4392
L_4 (nmol L^{-1})	−0.0101	0.4633	0.0980
Log K_4	−0.0637	0.3579	0.2125
Distance (km)	0.2328	−0.0769	0.1735

Although there was no clear pattern in the concentrations of ligands detected at each analytical window, the use of MAW highlighted the distinctions between the ligand pools in the surface and BBL. If only the $\alpha_{Fe(SA)_2} = 60$ window was used (as in most of the current electrochemical methods), subtleties in the patterns of L_1, L_3, and L_4 ligands may have been masked by not using an optimal analytical window. The contingency table produced for the chi-square analysis revealed that certain analytical windows were indeed optimized for the detection of a given ligand class based on the frequency of detections for that ligand class. These were also the same optimal windows predicted by using the ratio of log α_L : log $\alpha_{Fe(SA)_2}$ for determining the proper competition strength of the added ligand in CLE-ACSV titrations. The use of MAWs may therefore be most beneficial in dFe-binding ligand analysis with the use of targeted analytical windows depending on the ligand class of interest. Overall, MAW analysis enabled the detection of several distinct ligand classes, compared with previous studies.

Distributions of dFe-binding ligands—L_1 ligands: The strongest ligands measured in this study (L_1) were dominant in surface waters and along the continental shelf (Fig. 4A). L_1 detected in this study is similar in strength to the L_1 defined by Rue and Bruland (1995) in the North Pacific to be a siderophore-like ligand, where a similar analytical window was employed ($\alpha_{Fe(SA)_2} = 73$). The highest [L_1] and eL_1 ([L] − [Fe]) were observed in the regions influenced by riverine or estuarine input (San Francisco Bay, Eel River near Cape Mendocino), suggesting these areas are sources of strong dFe-binding ligands. Few studies have examined dFe-binding ligands in estuaries and rivers (Buck et al. 2007; Jones et al. 2011), but both

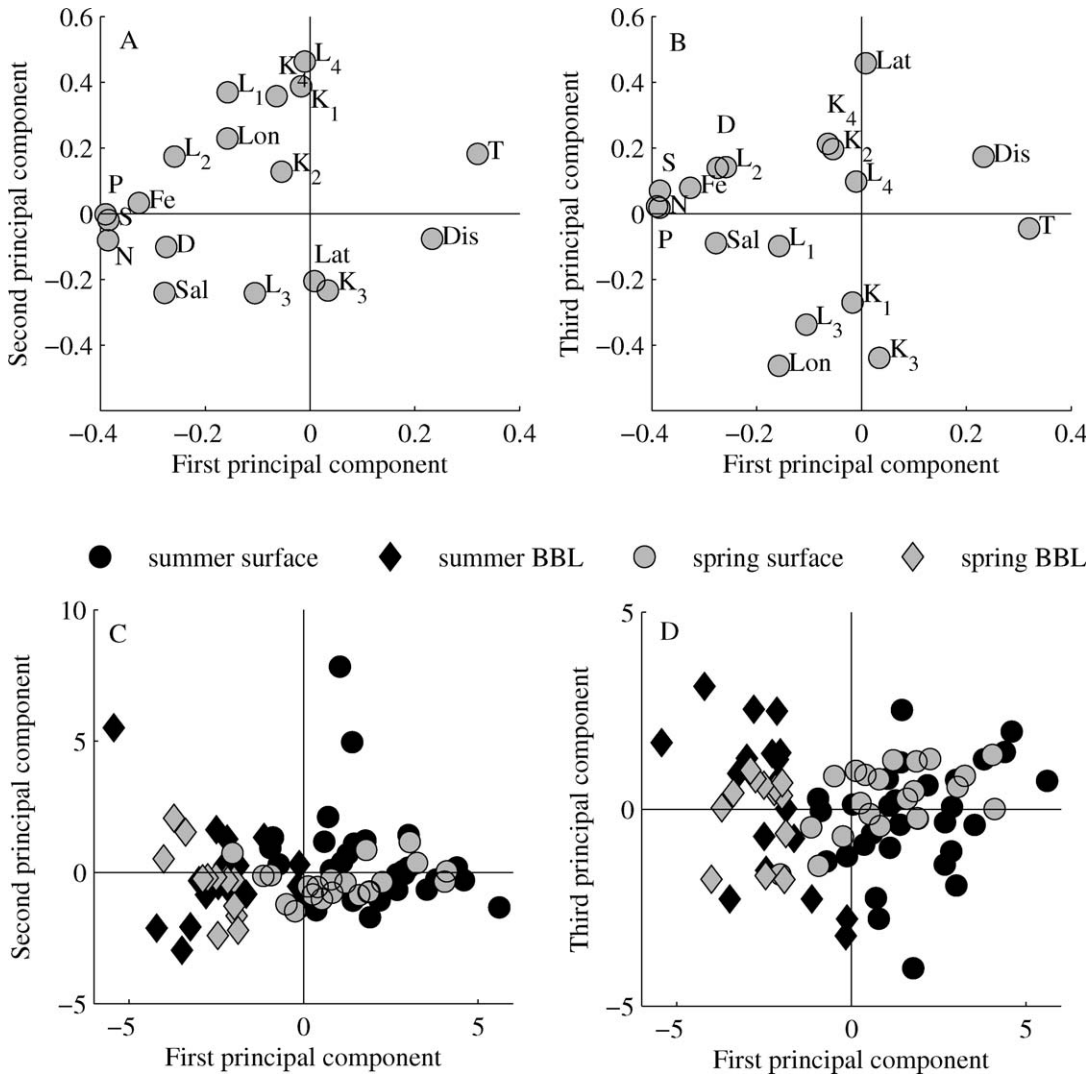

Fig. 6. The results of the principal component analysis (PCA) shown as scatter plots in the PC space. (A) PC loadings for the 18 variables used in PCA shown in the PCA space along the first PC (x-axis) and the second PC (y-axis). Variable labels are Lat (latitude), Lon (longitude), D (depth), T (temperature), Sal (salinity), N (nitrate), P (phosphate), S (silicate), Fe (dissolved Fe), L_1 ([L_1]), K_1 (log K_1), L_2 ([L_2]), K_2 (log K_2), L_3 ([L_3]), K_3 (log K_3), L_4 ([L_4]), K_4 (log K_4), and Dis (distance from shore). (B) PC loadings for the 18 variables used in the PCA along the first (x-axis) and third (y-axis) PCs. (C) The PCA scores of all of the data from each sample (82 samples) along the first and second PCs. (D) The PCA scores of all of the data from each sample along the first and third PCs.

detected high concentrations of dFe-binding ligands in freshwater-influenced systems. Buck et al. (2007) found elevated [L_1] in waters influenced both by the Columbia River Plume (north of this study) and San Francisco Bay. Buck et al. (2007) found a strong correlation between [L_1] and [dFe] and attributed this to the stronger ligand pool "capping" [dFe] in this region despite high concentrations of leachable particulate Fe, which could otherwise contribute to the dFe inventory. [L_1] was in excess of [dFe] in almost all of the surface samples in this study, supporting the finding from Buck et al. (2007) that L_1 is largely responsible for limiting [dFe] in the region, at least in steady state conditions. [L_1] and eL_1 also decline markedly offshore (Fig. 7), suggesting a coastal source of these ligands.

Bacteria in both marine and freshwater systems are known to produce siderophores (Haygood et al. 1993; Butler 1998; Macrellis et al. 2001), with similar log $K^{\mathrm{cond}}_{\mathrm{FeL_1,Fe'}}$ as the L_1 class observed here. It is probable that terrestrial or in situ strong ligands from San Francisco Bay may be a source of stronger ligands to CC coastal waters. This is an interesting finding, considering previous studies have suggested that L_1 is likely produced in situ (Rue and Bruland 1995). Buck et al. (2010) and King et al. (2012) found excess L_1 production in bottle incubations when NO_3^- : dFe (μmol L^{-1} : nmol L^{-1}) were high (> 10), indicating potential Fe stress relative to NO_3^- (Bruland et al. 1991; King and Barbeau 2007; Biller et al. 2013). Coastal samples in this study had very high NO_3^- : dFe ratios (up to 92 μmol L^{-1} : nmol L^{-1}) due to elevated NO_3^- during upwelling conditions and relatively low dFe. In fact, some of the samples with the highest NO_3^- : dFe ratios were associated with high eL_1 concentrations (data not shown).

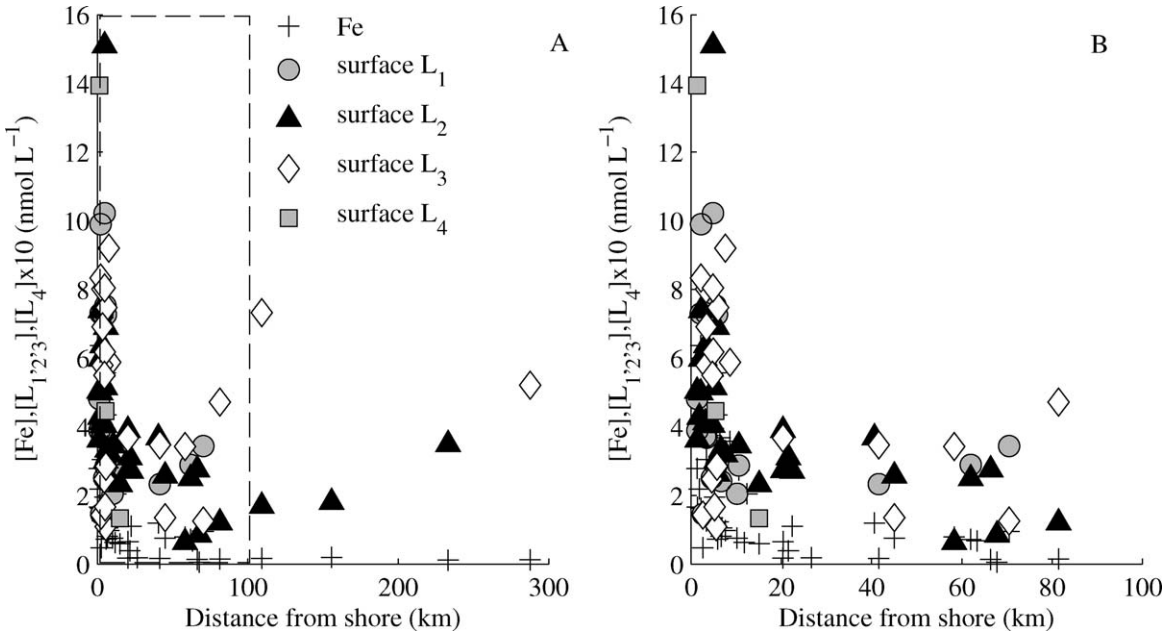

Fig. 7. The concentrations of Fe, L_1, L_2, L_3, and L_4 ($\times 10$) with distance from shore in all surface samples from the (A) spring and summer, and zoomed in to (B) 0–100 km offshore.

Macrellis et al. (2001) isolated strong dFe-binding ligands with known siderophore-like functional groups from this region, thus supporting their presence in the CC. L_1 ligands were also detected in some of the BBL samples (Table 2), although much less frequently than in the surface (7% of the BBL samples vs. 29% of the surface samples). This implies L_1 may also have a sediment source (Jones et al. 2011) or may reach the BBL without degradation. The presence of stronger ligands in the BBL may therefore play an important role in stabilizing dFe in this high-Fe environment.

Although L_1 might have a coastal source, it may also have an offshore sink. The decline in L_1 offshore could be due to degradation processes as coastal waters are advected offshore, resulting in the disappearance of L_1 and an increase in other ligand classes. The photochemical and biological degradation of L_1 has been hypothesized by several authors (Hutchins and Bruland 1994; Barbeau et al. 1996; *see* photochemical review by Barbeau 2006) but has only been documented in a few field studies (Powell and Wilson-Finelli 2003*a*,*b*; Rijkenberg et al. 2006). When L_1 ligand concentrations in surface nearshore waters (on the continental shelf) were compared with surface offshore waters from both cruises in this study, the samples were shown to be significantly different (chi-square, $p < 0.025$). This study presents indirect evidence that L_1 has a coastal source and is degraded as water masses move offshore.

L_2 ligands: L_2 ligands showed a similar spatial distribution to L_1, although L_2 was detected more often in offshore waters and in the BBL (Figs. 4B, 5). Although L_2 concentrations (and eL_2) declined offshore, they were still detected in the furthest offshore stations (Fig. 7). L_2, as defined in this study, is still part of the stronger ligand pool and, as such, may have sources similar to L_1. Few studies examining dFe-binding ligands in the marine environment have detected stronger ligands than the L_2 measured in this study, but most studies detect L_2 throughout the water column (*see* review by Gledhill and Buck 2012). This may be related to the analytical window used in the analyses, since a higher window was used in this study and also in Rue and Bruland (1995), who first suggested the presence of a stronger L_1 ligand class limited to surface waters in offshore environments. The L_2 ligand class defined here agrees with the majority of previous work, in that it was the most ubiquitous ligand class measured in this region. L_2 was found both in surface waters and the BBL and has elevated concentrations over the wide continental shelf dominated by mud flats (Wheatcroft et al. 1997).

Although CLE-ACSV gives no information on the structure of the ligands detected, additional analyses for HS in this study give some evidence that the L_2 class is partly composed of HS. The log $K^{cond}_{FeL_{HS},Fe'}$ of HS has been determined to be 11.1 (Laglera et al. 2007) and would make it part of the L_2 ligand class in this work. HS analyses on selected samples from the BBL indicate that HS is one of the components of the BBL ligand pool, with 22.6 and 39.2 μg L^{-1} HS amounting to 3–18% of the complexation in the BBL in these samples (where only L_2 was detected). Terrestrially derived HS have been found in coastal and deep waters to contribute to the pool of dFe-binding ligands (up to 4% of the deep dissolved organic matter pool; Laglera and van den Berg 2009), and these results are in the range found by Laglera and van den Berg (2009) in deep waters of the Pacific (36 μg L^{-1}). Lower [HS] were observed in this study than those reported for the Irish Sea by Laglera and van den Berg (2009; 70–400 μg L^{-1}), yet HS still represented a portion of the dFe-binding ligand pool. Calculations for the percentage of the ligand pool composed of HS were completed using a binding capacity for HS of 32 nmol L^{-1} Fe^{-1} : 1 mg HS determined by

Laglera and van den Berg (2009). The binding capacity of HS may vary widely; preliminary results in this study showed that different batches of Suwannee River fulvic acid standard can bind anywhere from 12 to 32 nmol L^{-1} Fe mg^{-1} HS (data not shown). Thus, 3–18% of the dFe binding in the BBL likely represents a lower bound on the binding capacity of HS in this system. These results represent some of the first definitive evidence that coastal margin sediments may be a source of HS and L_2 ligands.

L_3 and L_4 ligands: The distribution of weaker dFe-binding ligands is not well understood in the marine environment. This is partially due to analytical constraints, because studies to date have focused on siderophore-like ligands using stronger analytical windows (Rue and Bruland 1995) and the detection of weaker ligands is not as statistically robust as the stronger ligand class (Wu and Jin 2009). A lower analytical window was employed in this study to gain insight into the spatial distribution of weaker ligands in the surface and BBL, since they are hypothesized to play an important role in dFe cycling (Boyd et al. 2010) and phytoplankton iron acquisition (Hassler et al. 2011). Samples with the lowest temperatures in the surface and BBL tended to have the highest concentrations of weaker ligands, suggesting the source of most of the weaker ligands is the BBL or deeper waters. These samples also corresponded to stations with high [NO_3^-] and manganese (Mn) concentrations (Ana Aguilar-Islas pers. comm.; Biller and Bruland 2013), which supports the BBL as a source of weaker ligands since Mn concentrations are higher in areas influenced by reducing processes in margin sediments (Johnson et al. 1992; Biller and Bruland 2013). Diffusive fluxes of Cu-binding ligands have been found in estuary environments (Skrabal et al. 1997), implying a similar process could be occurring for dFe-binding ligands (Jones et al. 2011).

The highest concentrations of L_3 and L_4 ligands were detected in BBL samples in the mud belt regions of the continental margin (Fig. 5), known to be areas of high organic matter content and particulate Fe (Homoky et al. 2012). These L_3 and L_4 may thus represent organic by-products associated with organic matter degradation in margin sediments. Although it is not entirely clear what comprises this weaker ligand pool, it is likely a combination of degraded cellular material from surface waters (Hunter and Boyd 2007) like polysaccharides (Hassler et al. 2011), thiols (Dupont et al. 2006), or heme (Hopkinson et al. 2008). Evidence from surface waters supports the hypothesis that the weaker ligand pool comprises terrestrial and in situ degradation products as well. The L_3 and L_4 ligand classes both show distinct patterns offshore compared with L_1 and L_2 (Fig. 7). L_4 is only present in the stations closest to shore (< 25 km; Fig. 7B) and then quickly disappears offshore, suggesting scavenging of dFe and L_4 offshore and a nearshore source. The samples collected in the mouth of San Francisco Bay have the highest concentrations of L_4 ligands, indicating San Francisco Bay is likely a dominant source. On the other hand, L_3 ligands are the only class of ligands in this study that increase in concentration offshore (Fig. 7), despite the decline in dFe, strongly suggesting L_3 is related to degradation processes, perhaps of the L_1 and L_2 classes (Fig. 7). Stronger ligands may be degraded in surface waters by photochemistry (Barbeau 2006) or bacterial particle regeneration (Boyd et al. 2010), which have both been shown to produce weaker dFe-binding ligands best described by the L_3 class in this study.

Characteristics of the Fe-binding ligand pool in surface and BBL waters—The surface waters in this study were shown to contain a continuum of ligand classes, likely from terrestrial sources (HS from San Francisco Bay), the BBL (L_2, L_3, and L_4 ligands), and in situ production (L_1, L_2). This leads to heterogeneity of the surface ligand pool between samples that was difficult to explain by linear correlations alone (Pearson's correlation, data not shown), supporting results from the PCA that the variance in surface ligand distributions must be explained by several factors (Fig. 6). This finding is consistent with the hypothesis that a continuum of dFe-binding ligands likely exists in seawater as part of a heterogeneous dissolved organic carbon pool. Although the ligand classes are operationally defined in this study (based on the ligand strengths) and not necessarily ligands with different chemical structures, this analysis represents an initial step in determining the relevant processes governing complex ligand distributions in coastal waters.

The grouping of surface samples along the first PC in the PCA suggests a strong relationship with water masses in the CC, since the variance in the first PC is primarily explained by nutrient distributions. This result is supported by the onshore to offshore gradients in the ligand pool (Fig. 7), with the variance in surface waters explained predominantly by temperature, distance from shore, and nutrient concentrations (Fig. 7A,C). This result is not surprising, since previous evidence suggests numerous processes affect the dFe-binding ligand pool in surface waters (Gledhill and Buck 2012). The greater variance seen among surface samples is evidence that water mass–specific in situ processes are more important in surface samples than in the BBL, which exhibited relatively little variance between stations and seasons (Figs. 6, 7). Further evidence to suggest that the surface ligand pool is influenced by several sources and sinks is the different scale lengths of dFe and each ligand class as water masses advect offshore. Scale length can be defined as the distance at which the concentration has reached $1/e$ (37%) of its original concentration (here, concentration on the shelf; Johnson et al. 1997). The calculated scale length of dFe in surface waters from this study is 75 km, suggesting dFe is rapidly removed offshore. Each ligand class has scale lengths different from dFe, suggesting distinct processes influence their distributions and simple water mass mixing is not responsible for the patterns observed. Interestingly, L_1 and L_2 ligands have similar scale lengths of 133 and 187 km, respectively, whereas L_4 has a scale length of 6 km, and L_3 has a much longer scale length of 2000 km since it increases in concentration in many of the offshore stations. These scale lengths provide evidence that the excess ligand pools and dFe are largely decoupled in the CC, and complex patterns control their distributions. The longer persistence of ligands with distance from shore compared with dFe

may in part explain the higher deep-water dFe concentrations observed in the Pacific compared with the Atlantic (Johnson et al. 1997), if Pacific continental margin sediments are sources of both high [dFe] and ligands.

BBL samples show less variance than surface waters between samples and are predominantly grouped along the second and third PC. The low variance between BBL samples and their relationship to spatial parameters (latitude and longitude) suggest that ligands in the BBL are primarily related to their location on the shelf. The distribution of ligands on the shelf shows coherence with shelf width and dFe concentrations (Fig. 5), which have also been shown to be related to organic matter degradation processes (Homoky et al. 2012), as well as sediment type (Wheatcroft et al. 1997; Biller et al. 2013). The L_2 ligands were shown to be dominant in the BBL and were positively related to nutrient concentrations and L_1 (Pearson's correlation, data not shown). If the BBL ligand pool was directly related to degradation of the surface ligand pool, we would expect to see a negative trend between stronger (L_1 and L_2) and weaker ligands (L_3 and L_4) and a similar grouping of BBL and surface samples in the PC space. However, surface waters have much higher variance between samples, and the variance is explained by different factors from BBL samples. This is strong indirect evidence that the BBL ligand pool comprises material that has been deposited on the shelf from rivers and estuaries (Fig. 5) and from degradation processes in the sediments.

The surface and BBL are two very distinct biogeochemical regimes in the coastal ocean and provided good contrast for which to explore the use of MAW analysis for dFe speciation. The highest analytical window was optimal for characterizing the strongest Fe-binding ligands, whereas lower windows facilitated the detection of weaker ligands whose nature is poorly understood and often go undetected by current single-window methods. The MAW approach to dFe speciation in this study helped to determine the full spectrum of iron ligands and may be an important tool in future studies looking at the cycling of ligands in the marine environment. The ability to define a wider range of ligands with this analysis may also be helpful for future modeling efforts, where ligands are often poorly defined but important to overall dFe dynamics (Moore et al. 2004; Tagliabue and Volker 2011; Jiang et al. 2013). Future studies looking at mechanistic and temporal variations in the ligand pool will provide essential new information regarding the important role of dFe-binding ligands in Fe supply to productive coastal waters.

Acknowledgments

We thank Geoffrey Smith for help with sampling, the captain and crew of the R/V *Point Sur*, Tyler Coale for nutrient analyses, Ana Aguilar-Islas for manganese analyses, and Melissa Peacock for Chl *a* analyses. We also thank two anonymous reviewers and Mary Scranton for their helpful comments in improving the manuscript.

R.M.B. was supported by National Science Foundation (NSF) grant Division of Ocean Sciences (OCE) 10-26607 for the California Current Ecosystem Long Term Ecological Research program. This project was funded by NSF grant OCE 0849943 to K.W.B. and D.V.B. K.N.B. was supported by institutional funding from the Walwyn Hughes Fund for Innovation and the Ray Moore Endowment Fund at the Bermuda Institute of Ocean Sciences (BIOS).

This manuscript is BIOS contribution 2027.

References

Barbeau, K. 2006. Photochemistry of organic iron(III) complexing ligands in oceanic systems. Photochem. Photobiol. **82:** 1505–1516, doi:10.1111/j.1751-1097.2006.tb09806.x

———, J. W. Moffett, D. A. Caron, P. L. Croot, and D. L. Erdner. 1996. Role of protozoan grazing in relieving iron limitation of phytoplankton. Nature **380:** 61–64, doi:10.1038/380061a0

Berelson, W., and others. 2003. A time series of benthic flux measurements from Monterey Bay, CA. Cont. Shelf Res. **23:** 457–481, doi:10.1016/S0278-4343(03)00009-8

Biller, D. V., and K. W. Bruland. 2012. Analysis of Mn, Fe, Co, Ni, Cu, Zn, Cd, and Pb in seawater using the Nobias-chelate PA1 resin and magnetic sector inductively coupled plasma mass spectrometry (ICP-MS). Mar. Chem. **130:** 50–70.

———, and ———. 2013. Sources and distributions of Mn, Fe, Co, Ni, Cu, Zn, and Cd relative to macronutrients along the central California coast during the spring and summer upwelling season. Mar. Chem. **155:** 50–70, doi:10.1016/j.marchem.2013.06.003

———, T. H. Coale, G. J. Smith, and K. W. Bruland. 2013. Coastal iron and nitrate distributions during the spring and summer upwelling season in the central California Current upwelling regime. Cont. Shelf Res. **66:** 58–72, doi:10.1016/j.csr.2013.07.003

Boyd, P. W., E. Ibisanmi, S. G. Sander, K. A. Hunter, and G. A. Jackson. 2010. Remineralization of upper ocean particles: Implications for iron biogeochemistry. Limnol. Oceanogr. **55:** 1271–1288, doi:10.4319/lo.2010.55.3.1271

Bruland, K. W., J. R. Donat, and D. A. Hutchins. 1991. Interactive influences of bioactive trace-metals on biological production in oceanic waters. Limnol. Oceanogr. **36:** 1555–1577, doi:10.4319/lo.1991.36.8.1555

———, E. L. Rue, J. R. Donat, S. A. Skrabal, and J. W. Moffett. 2000. Intercomparison of voltammetric techniques to determine the chemical speciation of dissolved copper in a coastal seawater sample. Anal. Chim. Acta **405:** 99–113, doi:10.1016/S0003-2670(99)00675-3

———, ———, and G. J. Smith. 2001. Iron and macronutrients in California coastal upwelling regimes: Implications for diatom blooms. Limnol. Oceanogr. **46:** 1661–1674, doi:10.4319/lo.2001.46.7.1661

———, ———, ———, and G. R. DiTullio. 2005. Iron, macronutrients and diatom blooms in the Peru upwelling regime: Brown and blue waters of Peru. Mar. Chem. **93:** 81–103, doi:10.1016/j.marchem.2004.06.011

Buck, K. N., and K. W. Bruland. 2005. Copper speciation in San Francisco Bay: A novel approach using multiple analytical windows. Mar. Chem. **96:** 185–198, doi:10.1016/j.marchem.2005.01.001

———, M. C. Lohan, C. J. M. Berger, and K. W. Bruland. 2007. Dissolved iron speciation in two distinct river plumes and an estuary: Implications for riverine iron supply. Limnol. Oceanogr. **52:** 843–855, doi:10.4319/lo.2007.52.2.0843

———, J. Moffett, K. A. Barbeau, R. M. Bundy, Y. Kondo, and J. Wu. 2012. The organic complexation of iron and copper: An intercomparison of competitive ligand exchange–adsorptive cathodic stripping voltammetry (CLE-ACSV) techniques. Limnol. Oceanogr.: Methods **10:** 496–515, doi:10.4319/lom.2012.10.496

———, K. E. Selph, and K. A. Barbeau. 2010. Iron-binding ligand production and copper speciation in an incubation experiment of Antarctic Peninsula shelf waters from the Bransfield Strait, Southern Ocean. Mar. Chem. **122:** 148–159, doi:10.1016/j.marchem.2010.06.002

Bundy, R. M., K. Barbeau, and K. N. Buck. 2013. Sources of strong copper-binding ligands in Antarctic Peninsula surface waters. Deep-Sea Res. II **90:** 134–146, doi:10.1016/j.dsr2.2012.07.023

Butler, A. 1998. Acquisition and utilization of transition metal ions by marine organisms. Science **281:** 207–210, doi:10.1126/science.281.5374.207

Chase, Z., K. S. Johnson, V. A. Elrod, J. N. Plant, S. E. Fitzwater, L. Pickell, and C. M. Sakamoto. 2005. Manganese and iron distributions off central California influenced by upwelling and shelf width. Mar. Chem. **95:** 235–254, doi:10.1016/j.marchem.2004.09.006

Dupont, C. L., J. W. Moffett, R. R. Bidigare, and B. A. Ahner. 2006. Distributions of dissolved and particulate biogenic thiols in the subarctic Pacific Ocean. Deep-Sea Res. I **53:** 1961–1974, doi:10.1016/j.dsr.2006.09.003

Elrod, V. A., W. M. Berelson, K. H. Coale, and K. S. Johnson. 2004. The flux of iron from continental shelf sediments: A missing source for global budgets. Geophys. Res. Lett. **31:** L12307, doi:10.1029/2004GL020216

———, K. S. Johnson, S. E. Fitzwater, and J. N. Plant. 2008. A long-term, high-resolution record of surface water iron concentrations in the upwelling-driven central California region. J. Geophys. Res. C Oceans **113:** C11021, doi:10.1029/2007JC004610

Garnier, C., I. Pizeta, S. Mounier, J. Y. Benaim, and M. Branica. 2004. Influence of the type of titration and of data treatment methods on metal complexing parameters determination of single and multi-ligand systems measured by stripping voltammetry. Anal. Chim. Acta **505:** 263–275, doi:10.1016/j.aca.2003.10.066

Gerringa, L. J. A., P. M. J. Herman, and T. C. W. Poortvliet. 1995. Comparison of the linear van den Berg Ružić transformation and a nonlinear fit of the Langmuir isotherm applied to Cu speciation data in the estuarine environment. Mar. Chem. **48:** 131–142, doi:10.1016/0304-4203(94)00041-B

Gledhill, M., and K. N. Buck. 2012. The organic complexation of iron in the marine environment: A review. Front. Microbiol. **3:** 69–86.

Hassler, C. S., E. Alasonati, C. A. M. Nichols, and V. I. Slaveykova. 2011. Exopolysaccharides produced by bacteria isolated from the pelagic Southern Ocean—role in Fe binding, chemical reactivity, and bioavailability. Mar. Chem. **123:** 88–98, doi:10.1016/j.marchem.2010.10.003

Hawkes, J. A., M. Gledhill, D. P. Connelly, and E. P. Achterberg. 2013. Characterisation of iron binding ligands in seawater by reverse titration. Anal. Chim. Acta **766:** 53–60, doi:10.1016/j.aca.2012.12.048

Haygood, M. G., P. D. Holt, and A. Butler. 1993. Aerobactin production by a planktonic marine *Vibrio* sp. Limnol. Oceanogr. **38:** 1091–1097, doi:10.4319/lo.1993.38.5.1091

Homoky, W. B., S. Severmann, J. McManus, W. M. Berelson, T. E. Riedel, P. J. Statham, and R. A. Mills. 2012. Dissolved oxygen and suspended particles regulate the benthic flux of iron from continental margins. Mar. Chem. **134:** 59–70, doi:10.1016/j.marchem.2012.03.003

Hopkinson, B. M., K. L. Roe, and K. A. Barbeau. 2008. Heme uptake by *Microscilla marina* and evidence for heme uptake systems in the genomes of diverse marine bacteria. Appl. Environ. Microbiol. **74:** 6263–6270, doi:10.1128/AEM.00964-08

Hudson, R. J. M., D. T. Covault, and F. M. M. Morel. 1992. Investigations of iron coordination and redox reactions in seawater using Fe-59 radiometry and ion-pair solvent-extraction of amphiphilic iron complexes. Mar. Chem. **38:** 209–235, doi:10.1016/0304-4203(92)90035-9

———, E. L. Rue, and K. W. Bruland. 2003. Modeling complexometric titrations of natural water samples. Environ. Sci. Technol. **37:** 1553–1562, doi:10.1021/es025751a

Hunter, K. A., and P. W. Boyd. 2007. Iron-binding ligands and their role in the ocean biogeochemistry of iron. Environ. Chem. **4:** 221–232, doi:10.1071/EN07012

Hutchins, D. A., and K. W. Bruland. 1994. Grazer-mediated regeneration and assimilation of Fe, Zn and Mn from planktonic prey. Mar. Ecol. Prog. Ser. **110:** 259–269, doi:10.3354/meps110259

———, G. R. DiTullio, Y. Zhang, and K. W. Bruland. 1998. An iron limitation mosaic in the California upwelling regime. Limnol. Oceanogr. **43:** 1037–1054, doi:10.4319/lo.1998.43.6.1037

Ibisanmi, E., S. G. Sander, P. W. Boyd, A. R. Bowie, and K. A. Hunter. 2011. Vertical distributions of iron-(III) complexing ligands in the Southern Ocean. Deep-Sea Res. II **58:** 2113–2125, doi:10.1016/j.dsr2.2011.05.028

Jiang, M., K. A. Barbeau, K. E. Selph, K. N. Buck, F. Azam, B. Mitchell, and M. Zhou. 2013. The role of organic ligands in iron cycling and primary productivity in the Antarctic Peninsula: A modeling study. Deep-Sea Res. II **90:** 112–133, doi:10.1016/j.dsr2.2013.01.029

Johnson, K. S., and others. 1992. Manganese flux from continental-margin sediments in a transect through the oxygen minimum. Science **257:** 1242–1245, doi:10.1126/science.257.5074.1242

———, F. P. Chavez, V. A. Elrod, S. E. Fitzwater, J. T. Pennington, K. R. Buck, and P. M. Walz. 2001. The annual cycle of iron and the biological response in central California coastal waters. Geophys. Res. Lett. **28:** 1247–1250, doi:10.1029/2000GL012433

———, ———, and G. E. Friederich. 1999. Continental-shelf sediment as a primary source of iron for coastal phytoplankton. Nature **398:** 697–700, doi:10.1038/19511

———, R. M. Gordon, and K. H. Coale. 1997. What controls dissolved iron concentrations in the world ocean? Mar. Chem. **57:** 137–161, doi:10.1016/S0304-4203(97)00043-1

———, and others. 2007. Developing standards for dissolved iron in seawater. EOS Trans. Am. Geophys. Union **88:** 131–132, doi:10.1029/2007EO110003

Jones, M. E., J. S. Beckler, and M. Taillefert. 2011. The flux of soluble organic-iron(III) complexes from sediments represents a source of stable iron(III) to estuarine waters and to the continental shelf. Limnol. Oceanogr. **56:** 1811–1823, doi:10.4319/lo.2011.56.5.1811

King, A. L., and K. Barbeau. 2007. Evidence for phytoplankton iron limitation in the southern California Current System. Mar. Ecol. Prog. Ser. **342:** 91–103, doi:10.3354/meps342091

———, K. N. Buck, and K. A. Barbeau. 2012. Quasi-Lagrangian drifter studies of iron speciation and cycling off Point Conception, California. Mar. Chem. **128:** 1–12, doi:10.1016/j.marchem.2011.11.001

Kogut, M. B., and B. M. Voelker. 2001. Strong copper-binding behavior of terrestrial humic substances in seawater. Environ. Sci. Technol. **35:** 1149–1156, doi:10.1021/es0014584

Laglera, L. M., G. Battaglia, and C. M. G. van den Berg. 2007. Determination of humic substances in natural waters by cathodic stripping voltammetry of their complexes with iron. Anal. Chim. Acta **599:** 58–66, doi:10.1016/j.aca.2007.07.059

———, ———, AND ———. 2011. Effect of humic substances on the iron speciation in natural waters by CLE/CSV. Mar. Chem. **127:** 134–143, doi:10.1016/j.marchem.2011.09.003

———, J. DOWNES, AND J. SANTOS-ECHEANDÍA. 2013. Comparison and combined use of linear and non-linear fitting for the estimation of complexing parameters from metal titrations of estuarine samples. Mar. Chem. **155:** 102–112, doi:10.1016/j.marchem.2013.06.005

———, AND C. M. G. VAN DEN BERG. 2009. Evidence for geochemical control of iron by humic substances in seawater. Limnol. Oceanogr. **54:** 610–619, doi:10.4319/lo.2009.54.2.0610

LIU, X. W., AND F. J. MILLERO. 2002. The solubility of iron in seawater. Mar. Chem. **77:** 43–54, doi:10.1016/S0304-4203(01)00074-3

LOHAN, M. C., A. M. AGUILAR-ISLAS, AND K. W. BRULAND. 2006. Direct determination of iron in acidified (pH 1.7) seawater samples by flow injection analysis with catalytic spectrophotometric detection: Application and intercomparison. Limnol. Oceanogr.: Methods **4:** 164–171, doi:10.4319/lom.2006.4.164

MACRELLIS, H. M., C. G. TRICK, E. L. RUE, G. SMITH, AND K. W. BRULAND. 2001. Collection and detection of natural iron-binding ligands from seawater. Mar. Chem. **76:** 175–187, doi:10.1016/S0304-4203(01)00061-5

MANTOURA, R. F. C., AND J. P. RILEY. 1975. Analytical concentration of humic substances from natural-waters. Anal. Chim. Acta **76:** 97–106, doi:10.1016/S0003-2670(01)81990-5

MOFFETT, J. W., L. E. BRAND, P. L. CROOT, AND K. A. BARBEAU. 1997. Cu speciation and cyanobacterial distribution in harbors subject to anthropogenic Cu inputs. Limnol. Oceanogr. **42:** 789–799, doi:10.4319/lo.1997.42.5.0789

MOORE, J. K., S. C. DONEY, AND K. LINDSAY. 2004. Upper ocean ecosystem dynamics and iron cycling in a global three-dimensional model. Glob. Biogeochem. Cycles **18:** Gb4028, doi:10.1029/2004gb002220

NDUNG'U, K. 2012. Model predictions of copper speciation in coastal water compared to measurements by analytical voltammetry. Environ. Sci. Technol. **46:** 7644–7652, doi:10.1021/es301017x

POORVIN, L., S. G. SANDER, I. VELASQUEZ, E. IBISANMI, G. R. LECLEIR, AND S. W. WILHELM. 2011. A comparison of Fe bioavailability and binding of a catecholate siderophore with virus-mediated lysates from the marine bacterium *Vibrio alginolyticus* PWH3a. J. Exp. Mar. Biol. Ecol. **399:** 43–47, doi:10.1016/j.jembe.2011.01.016

POWELL, R. T., AND A. WILSON-FINELLI. 2003*a*. Importance of organic Fe complexing ligands in the Mississippi River plume. Estuar. Coast. Shelf Sci. **58:** 757–763, doi:10.1016/S0272-7714(03)00182-3

———, AND ———. 2003*b*. Photochemical degradation of organic iron complexing ligands in seawater. Aquat. Sci. **65:** 367–374, doi:10.1007/s00027-003-0679-0

RIJKENBERG, M. J. A., L. J. A. GERRINGA, I. VELZEBOER, K. R. TIMMERMANS, A. G. J. BUMA, AND H. J. W. DE BAAR. 2006. Iron-binding ligands in Dutch estuaries are not affected by UV induced photochemical degradation. Mar. Chem. **100:** 11–23, doi:10.1016/j.marchem.2005.10.005

RUE, E. L., AND K. W. BRULAND. 1995. Complexation of iron(III) by natural organic-ligands in the central north pacific as determined by a new competitive ligand equilibration adsorptive cathodic stripping voltammetric method. Mar. Chem. **50:** 117–138, doi:10.1016/0304-4203(95)00031-L

RUŽIĆ, I. 1982. Theoretical aspects of the direct titration of natural-waters and its information yield for trace-metal speciation. Anal. Chim. Acta **140:** 99–113, doi:10.1016/S0003-2670(01)95456-X

SANDER, S. G., K. A. HUNTER, H. HARMS, AND M. WELLS. 2011. Numerical approach to speciation and estimation of parameters used in modeling trace metal bioavailability. Environ. Sci. Technol. **45:** 6388–6395, doi:10.1021/es200113v

SCATCHARD, G. 1949. The attractions of proteins for small molecules and ions. Ann. N. Y. Acad. Sci. **51:** 660–672, doi:10.1111/j.1749-6632.1949.tb27297.x

SKRABAL, S. A., J. R. DONAT, AND D. J. BURDIGE. 1997. Fluxes of copper-complexing ligands from estuarine sediments. Limnol. Oceanogr. **42:** 992–996, doi:10.4319/lo.1997.42.5.0992

TAGLIABUE, A., AND C. VOLKER. 2011. Towards accounting for dissolved iron speciation in global ocean models. Biogeosciences **8:** 3025–3039, doi:10.5194/bg-8-3025-2011

VAN DEN BERG, C. M. G. 1982. Determination of copper complexation with natural organic ligands in sea water by equilibration with manganese dioxide 1. Theory. Mar. Chem. **11:** 307–322, doi:10.1016/0304-4203(82)90028-7

———, AND J. R. DONAT. 1992. Determination and data evaluation of copper complexation by organic ligands in sea water using cathodic stripping voltammetry at varying detection windows. Anal. Chim. Acta **257:** 281–291, doi:10.1016/0003-2670(92)85181-5

———, M. NIMMO, P. DALY, AND D. R. TURNER. 1990. Effects of the detection window on the determination of organic copper speciation in estuarine waters. Anal. Chim. Acta **232:** 149–159, doi:10.1016/S0003-2670(00)81231-3

WHEATCROFT, R. A., C. K. SOMMERFIELD, D. E. DRAKE, J. C. BORGELD, AND C. A. NITTROUER. 1997. Rapid and widespread dispersal of flood sediment on the northern California margin. Geology **25:** 163–165, doi:10.1130/0091-7613(1997)025<0163:RAWDOF>2.3.CO;2

WU, J. F., AND M. B. JIN. 2009. Competitive ligand exchange voltammetric determination of iron organic complexation in seawater in two-ligand case: Examination of accuracy using computer simulation and elimination of artifacts using iterative non-linear multiple regression. Mar. Chem. **114:** 1–10, doi:10.1016/j.marchem.2009.03.001

WU, J., AND G. W. LUTHER III. 1995. Complexation of Fe (III) by natural organic ligands in the Northwest Atlantic Ocean by a competitive ligand equilibration method and a kinetic approach. Mar. Chem. **50:** 159–177, doi:10.1016/0304-4203(95)00033-N

Associate editor: Mary I. Scranton

Received: 21 August 2013
Accepted: 01 January 2014
Amended: 13 January 2014